# Concentration factors and biological half-lives for the dynamic modelling of radionuclide transfers to marine biota in the English Channel

Bruno Fiévet, Pascal Bailly Du Bois, Claire Voiseux

# Concentration factors and biological half-lives for dynamic modelling of radionuclide transfer to marine biota in the English Channel

Bruno Fiévet[1,*], Pascal Bailly du Bois[2] and Claire Voiseux[1]

[1]Laboratoire de Radioécologie de Cherbourg-Octeville, Institut de Radioprotection et de Sûreté Nucléaire/PSE-ENV/SRTE, Rue Max Pol Fouchet, BP10, 50130 Cherbourg-en-Cotentin, France.

[22]LUSAC-Intechmer, Conservatoire National des Arts et Métiers, Boulevard de Collignon, Tourlaville, 50110, Cherbourg-en-Cotentin, France.

Institut de Radioprotection et de Sûreté Nucléaire

FIEVET Bruno <bruno.fievet@irsn.fr>;
BAILLY DU BOIS Pascal <pascal.baillydubois@lecnam.net>;
VOISEUX Claire <claire.voiseux@irsn.fr>;

* Corresponding author.

Keywords: Radionuclide biokinetics; Transfer modelling; Concentration factor; Biological half-life; Marine environment

**ABSTRACT**

The biokinetics of radionuclide transfers to biota in the marine environment can be modelled using two parameters, specific to both each element/radionuclide and biota. The Concentration Factor (CF) reflects the ratio between the activity concentrations in the biota and the surrounding seawater in steady state. The biological half-life ($tb_{1/2}$) characterizes depuration kinetics for the radionuclide from the biota. While recommended CF values can be found in the literature, no guidelines actually exist for $tb_{1/2}$ values. We used available time-series activity concentration measurements in biota in the English Channel, where controlled amounts of liquid radioactive waste are discharged by the ORANO La Hague reprocessing plant. We calculated the corresponding time-series activity concentrations in seawater for each biota dataset using an extensively-validated hydrodynamic model. We derived the values of CF and $tb_{1/2}$ from seawater and biota data, to model radionuclide transfers between the two compartments. To assess the performance of the model, we analyzed the residual between observed and calculated levels in the biota. Datasets for macroalgae, mollusks, crustaceans and fish yielded parameters (CF, $tb_{1/2}$) for H-3 (as body water and as organically bound tritium), C-14, Sb-125, Cs-137, I-129, Mn-54, Co-60, Zn-65 and Ru-106. After discussing the results and qualifying the model's reliability, we proposed recommendations for CF and $tb_{1/2}$ for the purposes of the operational modelling of radionuclide transfers to biota in the marine environment.

## 1 Introduction

Controlled amounts of radionuclides are discharged into the marine environment by nuclear industry under regular operation. They add to the background level resulting from natural origin, fallouts from past nuclear weapon tests, nuclear accidents, and possibly medical use. Radionuclides are mandatorily monitored in the environment to check that the consequences of controlled discharges are consistent with the predictions made by the operators when they requested the authorizations from their national regulatory authorities. Monitoring programs focus on indicator compartments (seawater, sediment) and a selection of biota as bioindicators. Marine bioindicator species can be collected repeatedly all year long in the geographical area of interest, to follow the spatial and

temporal changes in relation to the discharges. Addressing radioprotection of human and the environment requires to estimate the activity concentrations in potentially all components of the environment. Radionuclide measurements in the natural medium for monitoring purpose or radioecology studies, are used to design transfer models to estimate the levels in other marine species.

Modelling radionuclide (Rn) transfer to biota in the marine environment is routinely implemented by considering that the concentration in the biota is proportional to that in seawater. According to eq. 1, the calculation consists in simply multiplying the concentration in seawater by a Concentration Factor (CF) value which is specific for the radionuclide and the biota of interest:

$$[Rn]_{biota} = CF_{(Rn,biota)} \,.\, [Rn]_{seawater} \qquad \text{eq. 1}$$

The CF is the ratio between the activity concentrations in the biota and seawater. CF values can be found in the literature but recommended consensual values for biota groups (seaweed, mollusk, crustacean and fish) are generally taken from IAEA Technical Reports Series (IAEA, 2004, 2014). So, as a prerequisite, estimation of activity concentrations in marine biota requires that the concentrations in seawater are known. This simple and convenient model assumes that the biota and seawater compartments are in steady state. However, depending on radionuclides, chemical form, species and many parameters, transfers between the two compartments takes time (Carvalho, 2018). There are many situations in the natural environment where the steady state assumption is not met because radionuclides inputs are not stable or environmental conditions vary (seasons, weather forcing). This includes in particular a close location to a source of controlled radionuclide discharges from a nuclear facility (discharges are usually not constant), or in the aftermath of an accidental release like the Fukushima-Daiichi nuclear power plant accident (FDNPP). Assuming a steady state inappropriately has two consequences: 1) When the seawater concentration rises, the activity in the biota is assumed to rise in parallel. Calculating the biota activity as the activity in seawater multiplied by the CF (eq. 1) is largely overestimating because the kinetics of the transfer actually results in a slower increase in the biota compared to seawater. 2) Conversely, when the activity in seawater drops (when the discharge stops or quickly declines), the biota progressively depurates so its activity decreases much slower than in seawater. Assuming it parallels that of seawater severely underestimates the activity in the biota. For example, if the radionuclide concentration in seawater returns rapidly to background level, assuming a steady state would mean that the concentration in the biota would also return to background at the same time. However, as an example, the many measurement data in fish after FDNPP accident showed that Cs137 persisted for a long time after it diluted in the Pacific Ocean water (Buesseler, 2012). Thus FDNPP accident raised the need to use biokinetic modelling to bring more realism to model predictions (Vives i Batlle *et al.*, 2018).

The biokinetics of transfer can be implemented in complex multi-compartments ecosystem models (Tateda *et al.*, 2013; Belharet *et al.*, 2016; Vives i Batlle, 2016), but they require many parameters which may not be available for all radionuclides and marine species. Another approach consists in considering only two interacting compartments, seawater and the biota. This 'two compartments' model still uses the concept of CF (which implements the ratio between the activity in the biota and in water in steady state) and adds another parameter, the biological half-life ($tb_{1/2}$) to implement the kinetics of the radionuclide transfer (Gomez, 1991). The 'two compartments' model is implemented as the following first order differential equation (eq. 2):

$$\frac{d[Rn]_{biota}}{dt} = k_{in}.[Rn](t)_{seawater} - k_{out}.[Rn](t)_{biota} \qquad \text{eq. 2}$$

with $[Rn]_{biota}$ = Rn activity concentration in the biota and $[Rn]_{seawater}$ = Rn activity concentration in seawater (as functions of time).
$CF_{(Rn,biota)} = k_{in}/k_{out}$ the concentration factor in steady state for the Rn and species of interest
$tb_{1/2}=Ln(2)/(k_{out}-k_p)$ the biological half-life for the Rn and species
$k_p$ = the radioactive decay of the Rn

This transfer between seawater and the biota (eq. 2) is implemented as a function of a time-series concentration in seawater as described in the Methods section 2.3.2 (eq. 3).

If the CF values can still be taken from the IAEA reports, there is actually no such recommendation for the values of $tb_{1/2}$. Some $tb_{1/2}$ values are available from the literature (see Gomez, 1991 and Beresford et al., 2015, for reviews). Many of them were determined in laboratory experimental condition which may not be suitable for use in the natural environment. An alternative approach consists in using time-series measurements in both seawater and biota, routinely carried out for monitoring purpose, to derive the values of CF and $tb_{1/2}$ (Fiévet *et al.*, 2003). A major benefit of this approach is that the biological half-life reflects all the environmental processes responsible for the transfer kinetics. This includes the direct seawater and the trophic routes with all sources of variation (age/size, food web, season, temperature, biological cycles, and so on). So it is particularly fit for the purpose of environment monitoring ?. For example, considering a population in an area of interest, individuals leaving the population for any reason (population dynamics) apparently contributes to the removal of the radionuclide from that local population. This removal reflects in periodic monitoring samplings within the local population because the activity in biota results from individual depuration as well as population renewal. This is particularly crucial for mobile species like fish and many other seafood species, but also true for fixed seaweed ripped during storms. The approach was already used in the marine environment for several radionuclides and species (Fiévet *et al.*, 2003; Fiévet *et al.*, 2006; 2013; 2017) and it relied on the availability of activity concentration time-series measurements in both seawater and biota. So far, the availability of radionuclide concentrations measurements in seawater has been a limitation but this latch is now released in the marine environment of the English Channel. French nuclear industry facilities have been discharging controlled amounts of radioactive liquid waste in the English Channel since the late 60'. The main contributor is the nuclear fuel reprocessing plant of ORANO La Hague (RP). There are also nuclear power plants (NPP) on the French coast at Flamanville, Paluel, Penly, Gravelines, and the NPP of Nogent-sur-Seine on the river Seine which flows into the English Channel. Thanks to the constant implementation of 'Best Applicable Techniques' (OSPAR Commission, 2014) by the operator, the amounts of discharges from the RP have declined by two orders of magnitude for most radionuclides since the 80' (ORANO, 2019). Those from each NPPs are two orders of magnitude below actual discharges from the RP (EDF, 2019). The British nuclear facilities on the South coast of the UK (Devonport, Winfrith and Dungeness) are also a small contribution to the liquid radioactive discharges in the English Channel (RIFE-25, 2019). The fate of the radioactive liquid discharges by the RP of ORANO La Hague was recently reviewed (Fiévet *et al.*, 2020). Radioactive discharges by the RP have been used as tracers to validate hydrodynamic models which nowadays reached a very good reliability (Bailly du Bois *et al.*, 2005; 2012; 2020). The chronicle of liquid discharges by the RP being known with a high time resolution, it is possible to estimate the concentration of radionuclides in seawater if they are assumed to spread as soluble substances (conservative radionuclides). Time-series changes in radionuclides concentrations in seawater can thus be calculated by the hydrodynamic tools at any location in the English Channel where times-series measurement data are available in biota. With time-series data available both in seawater and biota, it is possible to estimate the dynamic transfer parameters (CF and $tb_{1/2}$) between the two compartments using the data processing technique already used on the basis of measurements in seawater (Fiévet and Plet,

2003). Here the concentrations in seawater were not measured but they were calculated by the hydrodynamic model MARS-2D (Bailly du Bois *et al.*, 2005; 2012). Available radionuclide time-series measurements carried out by IRSN, ORANO La Hague and the French Navy for monitoring purpose or radioecology studies were identified back from the mid-80' up to 2016 in seaweed, mollusk, crustacean and fish and the corresponding time-series in seawater were calculated by the hydrodynamic model. This study reports the results of CF and $tb_{1/2}$ values estimation for soluble radionuclide dynamic transfer modelling in the English Channel, based on hydrodynamic modelling in seawater with MARS-2D. They included parameters for H3, C14, Sb125, I129 and Cs137, which could be considered to behave as soluble behaviour. Tentative estimation of transfer parameters was also carried out for Mn54, Co60, Zn65 and Ru106 with more or less success which are discussed. The results were reported for each radionuclide and individual species dataset as well as crunched by biota group (macroalgae, mollusk, crustacean and fish). Those transfer parameters can be used for implementing dynamic biota transfer modelling downstream seawater hydrodynamic modelling (Duffa *et al.*, 2016) or any other time-series data in seawater.

## 2 Material and method

### 2.1 Datasets

The datasets used in this paper are inventoried in a spreadsheet provided as supplementary material. For each time series, an identifier (#) is given with the radionuclide, the species, the sampling location, the time span of the sampling period, the number of concentration measurements and a comment when necessary. The identifier (#) is used throughout the paper to link the results with the individual datasets. Here is an example:

Dataset #1: H3; macroalgae *Fucus serratus* (toothed wrack); sampling location: Goury (Long: -1.9490; lat: +49.7158); sampled between Nov-08 and Nov-11; Nb obs. = 37; comment: from Fiévet *et al.*, 2013. When the time-series in the biota has already been published (but not used with the corresponding time-series in seawater calculated with the model), the reference is given as a comment. Data provided by ORANO or the French navy are also quoted as a comment. Figure 1 shows a map with the sampling locations. Three sampling locations were given as fishing areas, called West Cotentin, North Cotentin and East Cotentin. They are local fishing areas used for radioactivity monitoring purpose and their central theoretical locations are indicated on the map.

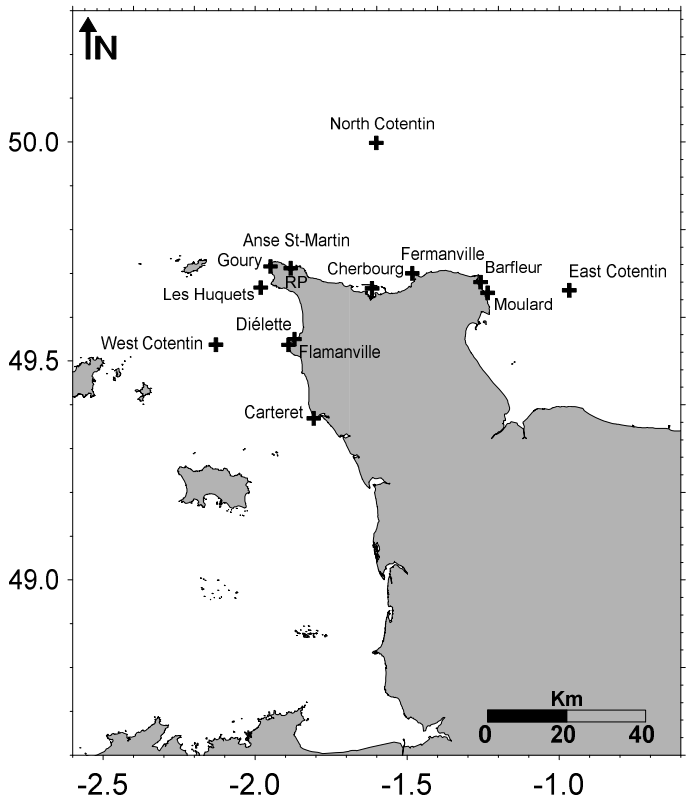


Figure 1: Map showing the ORANO La Hague reprocessing plant (RP) and the sampling locations of biota time-series measurements around the Cotentin peninsula.

For marine species potentially used in human seafood, the reported data corresponded to the edible parts (soft parts in mollusk, muscles in crustacean and fish).

Most available biota data were expressed in $Bq.Kg^{-1}$ dry weight. Average wet/dry weight ratios were used for conversion purpose since the CF corresponds to the activity in $Bq.Kg^{-1}$ wet in the biota, normalized to $Bq.Kg^{-1}$ in the water. In the present study, CF values correspond to $Bq.Kg^{-1}$ wet in biota per $Bq.L^{-1}$ in seawater, as in IAEA (2004). The conversion wet/dry weight ratios are given in the datasets inventory (supplementary material). In the event other wet/dry ratios would be preferred, scaling the CF values reported in the present paper is possible using the relationship:

$$\text{Preferred CF} = \text{present CF} * \text{preferred Ratio}_{w/d} / \text{present Ratio}_{w/d} \quad \text{eq. 4}$$

H3 biota data were split into H3 in the forms of organism' water (HTO) and organically bound tritium (OBT). Available HTO time-series were expressed in $Bq.L^{-1}$ and corresponding OBT time-series were expressed in $Bq.L^{-1}$ of combustion water (Fiévet *et al.*, 2013). They were kept unchanged, so the resulting CF values should be used accordingly. Unlike other radionuclides, the derived CF values yield activity concentrations in biota HTO in $Bq.L^{-1}$ and OBT in $Bq.L^{-1}$ combustion water (cw) and not in $Bq.Kg^{-1}$ wet. Conversion of $Bq.L^{-1}$ (cw) into $Bq.Kg^{-1}$ wet involves H% content of dry material and wet/dry ratio as described in Maro *et al.*, (2017).

Some of the available C14 biota data were expressed in $Bq.Kg^{-1}$ C and the necessary C content values needed for conversion are given in % dry weight in the datasets inventory (supplementary material).

In a few cases two different datasets for the same radionuclide/species/location were considered because the spans of the sampling periods were separated by an interval of several years. This provided an opportunity to test whether the transfer parameters values derived from the first one and the second one were consistent, several years apart. In some time-series, the periodicity was too long to derive $tb_{1/2}$ accurately but the data could be used anyway to check their consistency with $tb_{1/2}$ derived from other datasets with a shorter periodicity.

## 2.2 Hydrodynamic modelling

Radionuclide activity concentrations in seawater were calculated using the MARS-2D model previously described in (Bailly du Bois *et al.*, 2005, 2012, 2020 and references herein).The MARS-2D model uses two-dimensional horizontal approximation (i.e. shallow-water equations) capable of producing a satisfactory representation of dissolved-substance transport in the English Channel as demonstrated in references herein. These equations were solved using the finite-difference MARS model, with implicit alternate direction time-stepping for gravity-driven inertia waves. Non-linear terms were discretized semi-implicitly. Full details concerning the MARS algorithm are given by Lazure and Dumas (2008). The model used here involved a nesting strategy, starting from a broad region covering the entire North-West European continental shelf (with a 5.6-km grid resolution) down to a detailed domain covering the whole English Channel with a mesh size of 500 m. It accounted for real releases, tide and meteorological forcing to simulate instantaneous currents with a mean time step of 60 s. Real wind data were provided by Météo France and corresponded to the outputs from the European Centre for Medium-Range Weather model (The ERA-Interim reanalysis, 2011). Tide conditions were provided according to Lyard *et al.* (2006). The bathymetry was estimated from various data sources with the method described in Bailly du Bois *et al.*, (2005). Because the English Channel is shallow, the concentration is already homogeneous in the water column as close as 1 500 m from the outlet (Bailly du Bois *et al.*, 2020) which supports the use of a 2D model. Short- to long-term extensive validation of the model was carried out by model/measurements comparison as described in Bailly du Bois *et al.*, (2005, 2012, 2020). The releases fluxes from the RP were described and given available in Bailly du Bois *et al.*, (2020) and radioactive decay was implemented in the calculations.

## 2.3 Data processing

### *2.3.1 Building the corresponding time-series in seawater with the MARS-2D hydrodynamic model*

For each radionuclide, the MARS-2D hydrodynamic model was used to calculate the radionuclide concentrations in seawater in the English Channel with a space and time resolutions of 500 meters and 60 sec, respectively.. The calculated seawater concentrations were taken every 12 hours each day at 0h and 12h. When radionuclide discharges were only known as monthly amounts (C14, I129), the accuracy is lower, the space resolution was only 1 500 meters and the calculated concentrations were taken every 24 hours at 0h. The time-series concentration in seawater at the closest mesh to the biota sampling location was finally extracted from the 2D calculation results.

For C14, a constant background value for natural and other sources (fallouts from past atmospheric nuclear weapon tests) of 6.9 $Bq.L^{-1}$ was taken, corresponding to 249 $Bq.Kg^{-1}$ C in seawater dissolved inorganic carbon (DIC), according to Muir *et al.*, (2017).

For Cs137, a background value in the English Channel must also be added to account for the contribution of other sources of Cs-137 than the discharges from the RP. This background includes the fallouts from past nuclear weapon tests as well as Chernobyl accident and the contribution of discharges from Sellafield nuclear facilities (Irish Sea, UK). The potential contribution of dissolved radionuclide inputs coming from the Irish Sea and upstream of the general water mass flow from West to East in the English Channel was previously estimated by Bailly du Bois *et al.*, (1995; 2002).

This involved around 1% of discharges from Sellafield which was recently confirmed by Castrillejo *et al.*, (2020). The annual background values from 1966 to 2016 are given in the supplementary material.

For H3, the background level at the western entrance of the English Channel ranged between 0.07 and 0.33 $Bq.L^{-1}$ (Oms, 2018). It was considered negligible with respect to the levels around the Cotentin Peninsula (5 – 15 $Bq.L^{-1}$ ? Fiévet *et al.*, 2020). So, except for Cs137 and C14, no background correction was added to the seawater activity concentrations calculated by the MARS-2D model.

It should be pointed out that for mobile species (i.e. scallops, crustacean, fish …) the level of seawater concentration exposure was obviously a source of uncertainty due to seawater dispersion process. To attempt to reduce this bias, seawater concentrations were estimated as an average of 7 x 7 mesh (3.5 Km x 3.5 Km, centered on the theoretical sampling location). The averaging of 7 x 7 mesh was set arbitrarily for all mobile species though they may have various mobility behaviors.

In the cases of I129 and Co60, the distance (Km) between the outlet of the RP and the sampling locations were estimated as broken lines following average residual trajectories derived from Fiévet *et al.*, (2020). There are indicated in parenthesis in the tables of the Results section as appropriate.

### *2.3.2 Deriving the values of CF and $tb_{1/2}$ from datasets*

The values of the transfer parameters CF (steady state) and the biological half-life $tb_{1/2}$ were derived from times-series concentration in seawater and the biota as described in details in Fiévet and Plet, (2003). The time-series concentration in seawater was provided with a 12h (or 24h) periodicity so the calculated time-series in the biota had the same time resolution. The dynamic transfer model between seawater and the biota is implemented as eq. 3:

$$s_{(i)} = a.s_{(i-1)} + b.e_{(i)} \qquad \text{eq. 3}$$

$e_{(i)}$ = activity concentration in seawater calculated by the MARS-2D hydrodynamic model at step i (T = calculation time step, so time = i.T, which means every 0.5 or 1 day)
$s_{(i)}$ = activity concentration in the biota calculated by the transfer model at step i.
CF(steady state) = b/(1-a) (the concentration factor, as in eq. 1)
kp = radioactive decay ($d^{-1}$) for the Rn of interest
kb = -Ln(a)/T-kp ($d^{-1}$)
$tb_{1/2}$ = Ln(2)/kb (d) the biological half-life of the Rn for the biota of interest

It was then possible to compare the calculated and the observed values in the biota. Minimizing the residual between the two allowed estimating the optimal values of CF and $tb_{1/2}$. Two parameters (Rc and R) were calculated for each biota individual observation (Obs) and its corresponding value calculated by the transfer model (Mod), as described in Fiévet *et al.*, 2017.

If Mod < Obs then Rc = 1 – Obs/Mod else Rc = Mod/Obs - 1

The Rc value equals 0 when Mod and Obs exactly match, otherwise Mod and Obs were compared using their ratio yielding a relative residual. An absolute residual would have weight depending on the level but a relative residual can be compared for any observation whatever the radionuclide, the level, the time and so on. A histogram of Rc values could then be plotted with negative values corresponding to underestimation by the model and positive values to overestimation. Rc values histogram was expected to be centered as close as possible to 0 and symmetrical.

To further qualify the analysis of the relative residual, R was calculated as

R = Max [Obs/Mod; Mod/Obs]

R equals 1 when Mod and Obs exactly match. It is also a relative residual which can be compare for all observations in this study. The distribution of R values visualized as a histogram characterized the factor by which the model and the observations mismatched (whether the model under- or over-estimated). Minimizing the mean of the R values (R≥1) was a fitting criterion used here for determining the model parameters. Besides, the cumulative percentage of the distribution of R values allowed estimating the probability of the model mismatching by less than any factor.

R and Rc were also used in examples as criteria for model sensitivity analysis upon the parameters values.

For each analyzed dataset, the values of R and Rc were reported to score the residual between the MARSD-2D / Dynamic Transfer Model linked modelling and the observed values in the marine environment. Rmean and R95 (cumulative % = 95%) were given to account for the average mismatch factor and that of 95% observations, respectively. Rc median value (Rc50) gave the relative residual (positive or negative) between Mod and Obs (in %) for half the observations. The same scoring was reported for datasets merged by biota group.

## 3 Results

Two complete examples of dataset processing and results are presented for illustration purpose. Then the results from the entire database are sorted in tables by radionuclide and biota.

### 3.1 Examples of dataset processing

Dataset #24: Sb125 in the brown algae *Fucus vesiculosus* (bladder wrack) from Diélette illustrated the data processing in the context of a sessile species. Antimony was previously used as a tracer of soluble liquid discharge from the RP (Bailly du Bois *et al.*, 1995).

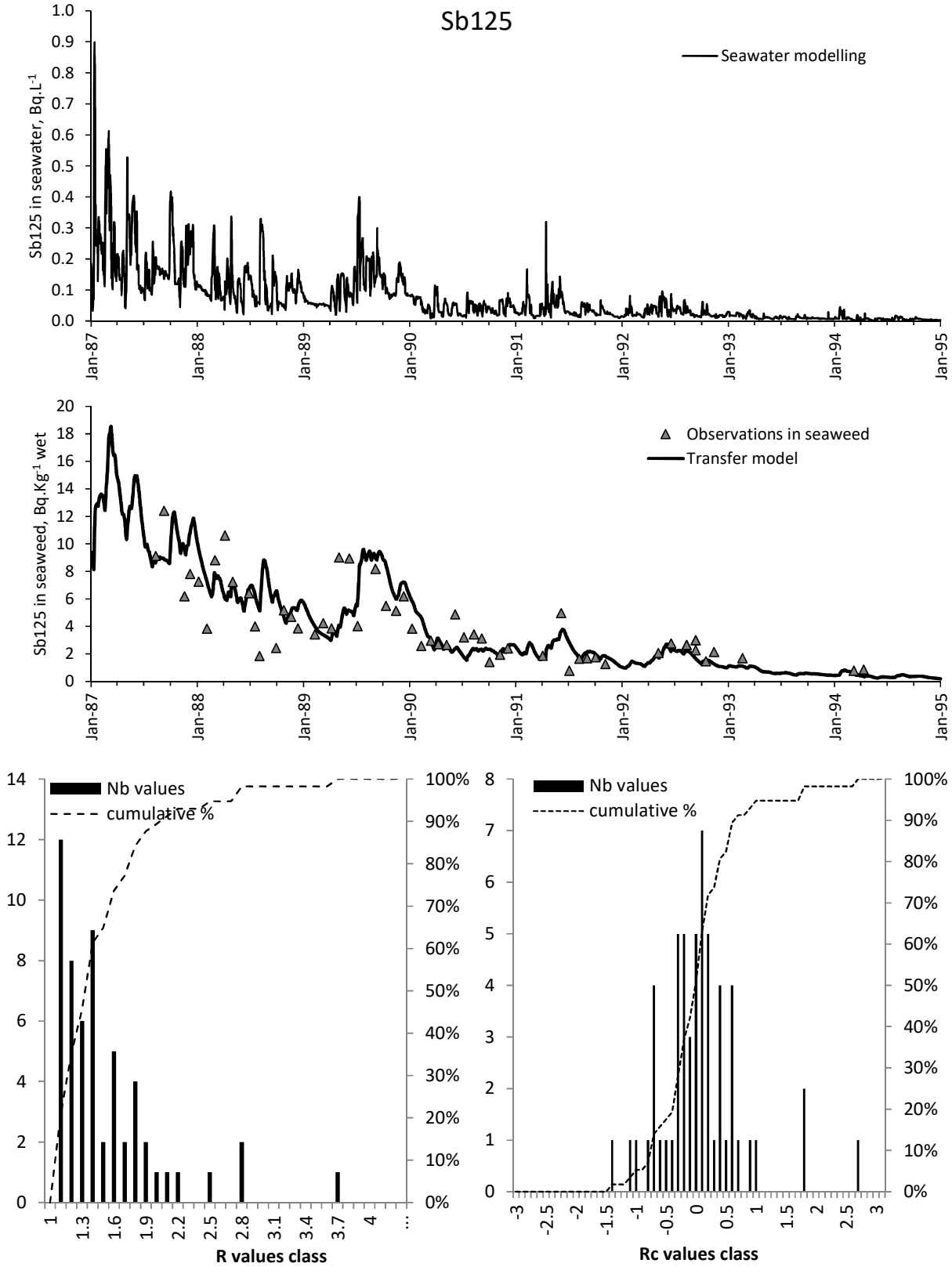


Figure 2: Dynamic transfer modelling of Sb125 between seawater and *Fucus vesiculosus* at Diélette (Figure 1). Top: Activity concentration in seawater calculated by the hydrodynamic model. Mid; Activity concentration observations (triangle symbols) and calculated by the transfer model (solid line) with CF = 56 $L.Kg^{-1}$ and $tb_{1/2}$ = 23 d. Bottom: Scoring of the overall modelling performance with

the distribution of the residual R and Rc values (see methods). Left: Histogram and cumulative percentage of R values. Right: Histogram and cumulative percentage of Rc values.

Minimal value of Rmean was obtained with CF = 56 and $tb_{1/2}$ = 23 d. Scoring the reliability of the model showed that the average mismatch ratio R between the predicted values (Mod) and the observations (Obs) was 1.47 and <2.8 in 95% of the 57 observations. The histogram of Rc values was centered on -0.01, which meant a trivial underestimation by 1%.

Dataset #68: Cs137 in round fish from the North Cotentin (data provided by ORANO) illustrated the data processing in the particularly challenging context of a mobile species, with high uncertainty on the seawater exposure levels. Geographical coordinates of the center of the sampling location were set to 1.60148 E; 50.20049 N (Figure 1) and seawater concentrations were estimated by averaging the values calculated by MARS-2D in a 3 500 m x 3 500 m area centered on that location.

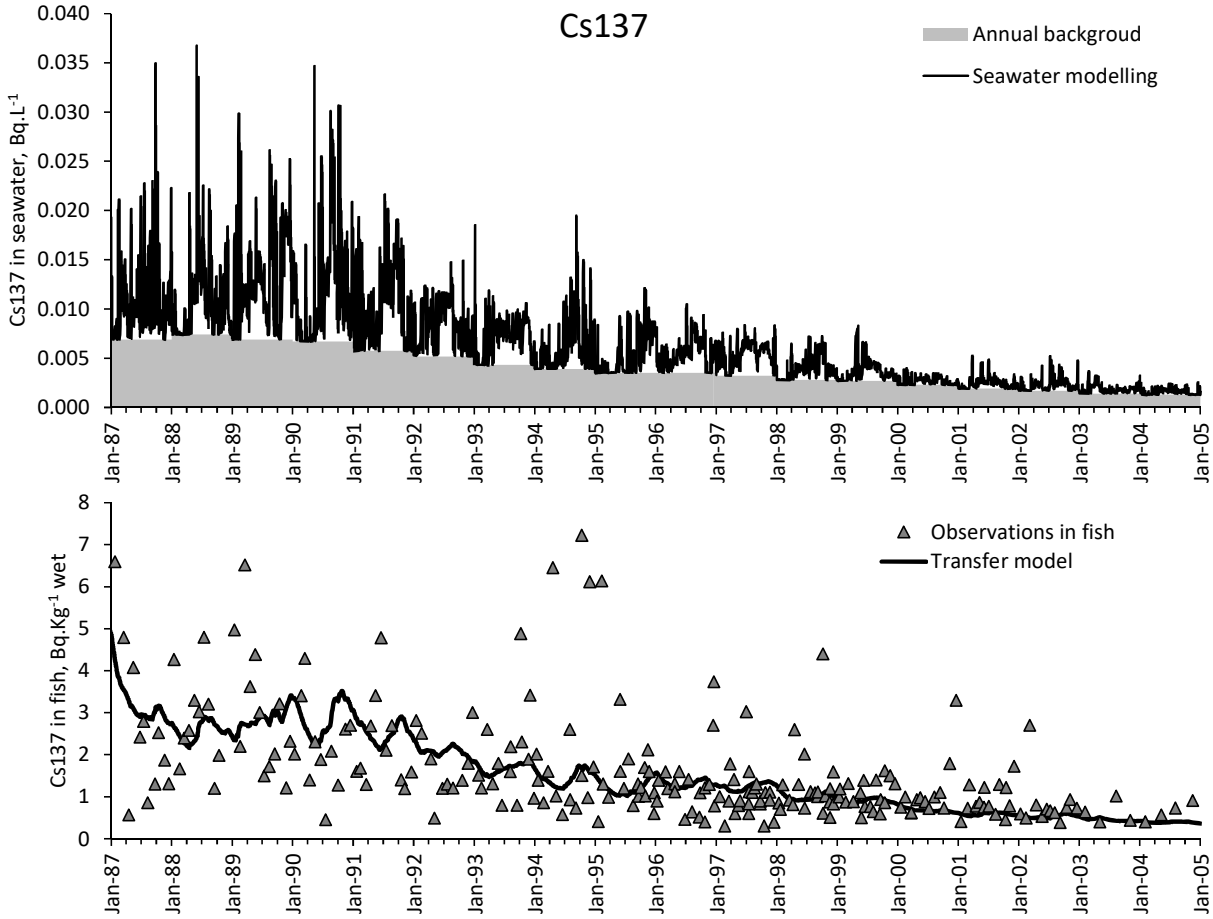

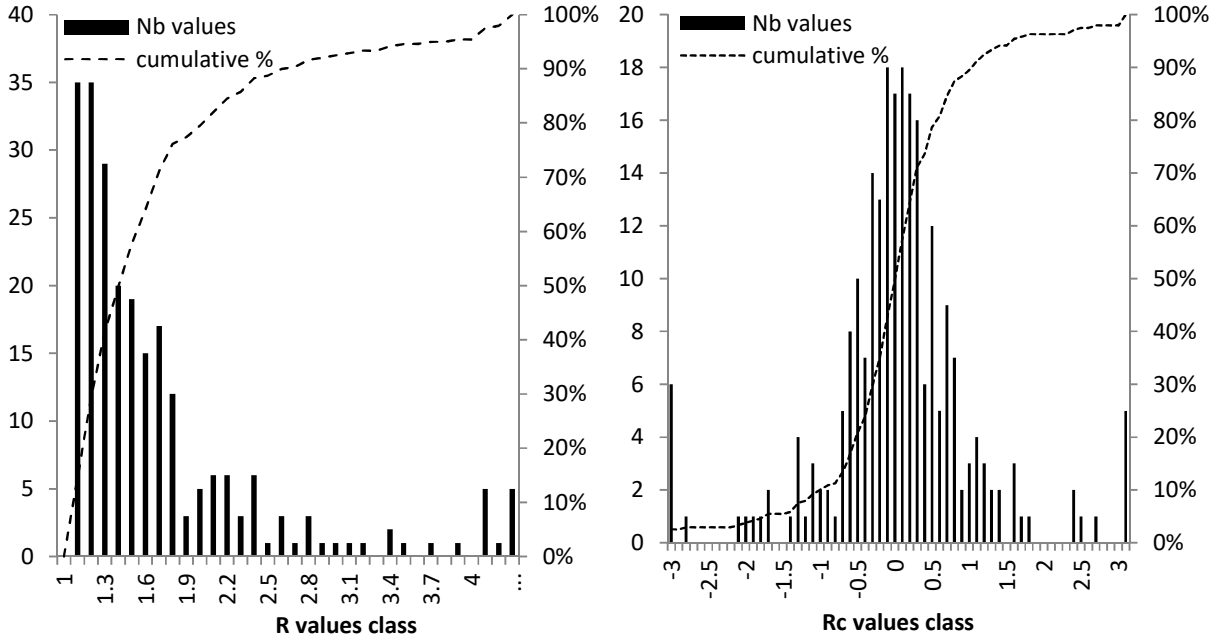


Figure 3: Dynamic transfer modelling of Cs137 between seawater and round fish caught at the 'North Cotentin' location (Figure 1). Top: Activity concentration in seawater calculated by the hydrodynamic model on the basis of liquid discharges from the RP. Shaded area: annual background level (see Section 2.3.1). Mid; Activity concentration observations (triangle symbols) and calculated by the transfer model (solid line) with CF = 57 ($L.Kg^{-1}$) and $tb_{1/2}$ = 71 d. Bottom: Scoring of the overall modelling performance with the distribution of the residual R and Rc values (see section 2.3.2). Left: Histogram and cumulative percentage of R values. Right: Histogram and cumulative percentage of Rc values.

Minimal value of Rmean was obtained with CF = 57 and $tb_{1/2}$ = 71 d. Scoring the reliability of the model showed that the average mismatch ratio R between the predicted values (Mod) and the observations (Obs) was 1.21 and <3.9 in 95% of the 239 observations. The histogram of Rc values was centered on +0.03, which meant a small overestimation by 3%. The histogram tails accounted for outliers out of the class ranges with R values up to 6.9 and Rc values spanning from -4.0 to +5.9. The cumulative % curves show that these outliers accounted for less than 5% observations.

R and Rc residual metrics provided an opportunity to carry out a sensitivity analysis of the values of the transfer parameters (CF and $tb_{1/2}$). The focus was put on $tb_{1/2}$ because the up and down shift of the calculated signal in biota directly depending on the value of CF was expectedly linear (data not shown; see discussion section 4.1). However, with the two examples shown above (sessile and mobile species), the R and Rc values were calculated with a range of $tb_{1/2}$ values to illustrate graphically the influence of $tb_{1/2}$ changes on the modelling performance.

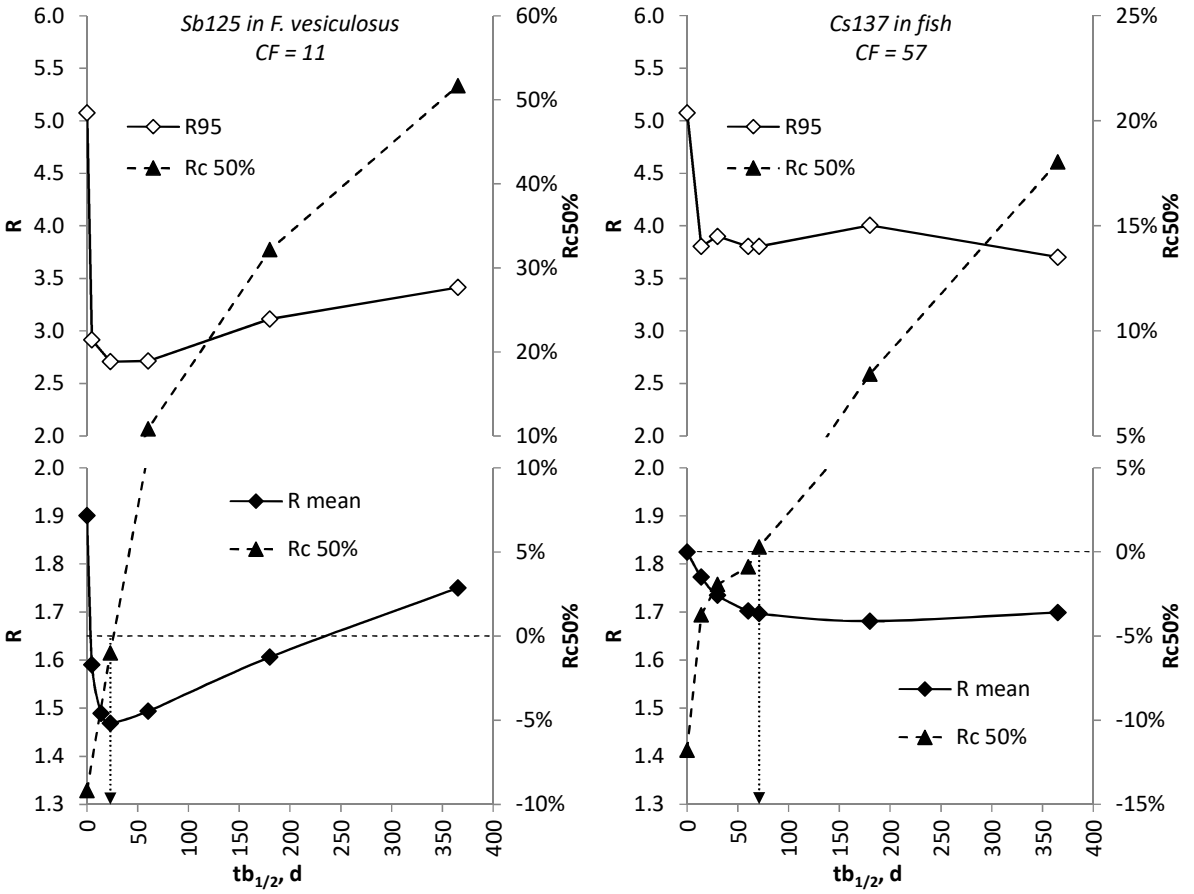


Figure 4: Sensitivity analysis of the modelling performance on the value of $tb_{1/2}$. Dependence of R (left axis; R mean: filled; R95: open diamonds) and Rc 50% (right axis; filled triangle) on the value of $tb_{1/2}$. Left panel: Sb125 in seaweed from Figure 2; right panel: Cs137 in fish from Figure 3. Left and right axis were broken to zoom on lower values of R mean and Rc50% on lower panels. The vertical arrows point at the optimal value retained for $tb_{1/2}$ corresponding to the combination of a minimal value of Rmean and a value of Rc50% close to zero.

In the case of Sb125 in *Fucus vesiculosus* (Figure 4, Left), the minimal value of R mean was used to select the optimal value of $tb_{1/2}$ of 23 days because the corresponding Rc50% value was close to zero. In the case of Cs137 in fish (Figure 4, right), with the high uncertainty related to mobile species, Rmean leveled off after it reached a minimal value. The Rc50% close to zero criterion was used to select the optimal value of $tb_{1/2}$ of 71 days.

### 3.2 Results for each individual dataset

The radionuclides were classified in two groups as soluble and non-soluble, as previously described in the context of discharges from the RP in the marine environment in the English Channel (Fiévet *et al.*, 2020). Soluble radionuclide spread out through water currents and their potential transfer to other compartments (biota and/or sediment) has little quantitative consequence on their concentrations in seawater.

Values of $tb_{1/2}$ in parenthesis indicate that the dataset was not used to derive this parameter. However, $tb_{1/2}$ was set arbitrarily, on the basis of its value derived from other similar datasets (see Discussion section).

Soluble radionuclides: H3, C14, Sb125, I129 and Cs137 were included in this category because they were expected to be soluble. We are aware that, due to its less soluble behaviour, previous Cs137

discharges potentially remobilized from sediment could interfere with hydrodynamic dilution of actual discharges.

Table 1: CF and $tb_{1/2}$ values derived for each individual dataset (Rn, species) and scoring results of the model for soluble radionuclides. The first occurrence of species names are preceded with a letter in parenthesis indicating the biota group (a: macroalgae; m: mollusk; c: crustacean; f: fish). CF values are expressed in $L.Kg^{-1}$ except for H3 (see Methods) and $tb_{1/2}$ values are in day.

| **Rn** | (Grp)**biota** | **nb Obs** | **CF** | **$tb_{1/2}$** | **Rmean** | **R95** | **Rc50(%)** | **dataset #** |
|---|---|---|---|---|---|---|---|---|
| H3 (HTO) | (a)*Fucus serratus* | 38 | 0.9 | 0.3 | 1.4 | 2.9 | +8.6 | *1* |
| | *Fucus serratus* | 31 | 0.9 | 0.3 | 1.5 | 2.0 | +8.3 | *2* |
| | (a)*Laminaria digitata* | 37 | 0.9 | 0.3 | 1.4 | 3.2 | +3.8 | *3* |
| | (m)*Patella sp* | 11 | 0.9 | 0.3 | 1.5 | 2.9 | +5.0 | *4* |
| | *Patella sp* | 26 | 1.0 | 0.3 | 1.4 | 2.0 | +2.5 | *5* |
| H3 (OBT) | *Fucus serratus* | 37 | 0.9 | 120 | 1.2 | 1.7 | -1.3 | *6* |
| | *Fucus serratus* | 31 | 0.9 | 110 | 1.3 | 2.2 | +1.7 | *7* |
| | *Fucus serratus* | 10 | 0.9 | (120) | 1.2 | 1.6 | +0.0 | *8* |
| | *Laminaria digitata* | 37 | 1.0 | 111 | 1.2 | 1.6 | -0.8 | *9* |
| | *Patella sp* | 9 | 1.0 | 195 | 1.1 | 1.5 | -2.5 | *10* |
| | *Patella sp* | 26 | 0.9 | 183 | 1.1 | 1.3 | +6.7 | *11* |
| | *Patella sp* | 5 | 1.0 | (120) | 1.3 | 2.2 | +5.0 | *12* |
| C14 | *Fucus serratus* | 36 | 3 454 | 56 | 1.1 | 1.3 | +0.0 | *13* |
| | *Fucus serratus* | 27 | 3 532 | 42 | 1.04 | 1.1 | -0.4 | *14* |
| | *Patella sp* | 28 | 4 090 | 108 | 1.02 | 1.1 | +1.8 | *15* |
| | *Patella sp* | 26 | 3 993 | 87 | 1.02 | 1.1 | +0.0 | *16* |
| | *Patella sp* | 8 | 3 127 | (120) | 1.03 | 1.1 | +0.0 | *17* |
| | (m)*Mytilus edulis* | 32 | 2 512 | 84 | 1.03 | 1.1 | +0.0 | *18* |
| | (c)*Homarus vulgaris* | 7 | 4 353 | 45 | 1.1 | 1.2 | -3.8 | *19* |
| | *Homarus vulgaris* | 6 | 3 601 | (45) | 1.1 | 1.4 | +0.0 | *20* |
| | (f)*Solea solea* | 8 | 4 675 | (120) | 1.1 | 1.2 | +0.0 | *21* |
| Sb125 | *Fucus serratus* | 87 | 10 | 49 | 1.5 | 2.7 | -0.5 | *22* |
| | *Fucus serratus* | 48 | 13 | (50) | 1.5 | 2.4 | -2.0 | *23* |
| | (a)*Fucus vesiculosus* | 57 | 11 | 23 | 1.5 | 2.8 | -2.5 | *24* |
| | *Patella sp* | 77 | 13 | (60) | 1.6 | 2.8 | +6.3 | *25* |
| | *Patella sp* | 79 | 8 | (60) | 1.5 | 2.9 | -2.8 | *26* |
| | *Patella sp* | 71 | 7 | 61 | 1.6 | 3.4 | +0.6 | *27* |
| | (m)*Pecten maximus* | 27 | 13 | (30) | 1.7 | 2.8 | -5.0 | *28* |
| | *Pecten maximus* | 18 | 8 | (30) | 1.4 | 2.9 | +10 | *29* |
| | *Mytilus edulis* | 46 | 3 | (30) | 1.6 | 2.6 | +5.0 | *30* |
| | (m)*Crassostrea gigas* | 28 | 3 | (30) | 1.6 | 2.9 | +5.0 | *31* |
| | (c)*Cancer pagurus* | 20 | 5 | 116 | 1.5 | 2.4 | +3.3 | *32* |
| | *Cancer pagurus* | 73 | 11 | 138 | 1.6 | 2.8 | +1.0 | *33* |
| I129 (dist./ outlet, Km) | *Fucus serratus* (6 Km) | 31 | 9 523 | (20) | 1.6 | 2.9 | -1.7 | *34* |
| | *Fucus serratus* (6 Km) | 63 | 11 783 | *17* | 1.5 | 2.3 | -1.3 | *35* |
| | *Fucus serratus* (6 Km) | 34 | 11 264 | 17 | 1.3 | 1.8 | +0.0 | *36* |
| | *Fucus serratus* (12 Km) | 6 | 4 948 | (*14*) | 1.2 | 1.6 | +0.0 | *37* |
| | *Fucus serratus* (45 Km) | 10 | 5 814 | 22 | 1.4 | 2.1 | +0.0 | *38* |
| | *Fucus serratus* (42 Km) | 10 | 4 365 | (*14*) | 1.6 | 2.4 | +0.0 | *39* |

| | | | | | | | | |
|---|---|---|---|---|---|---|---|---|
| | *Laminaria digitata* (6 Km) | 40 | 38 210 | (*14*) | 1.6 | 2.7 | +3.3 | *40* |
| | *Laminaria digitata* (27 Km) | 4 | 25 292 | (*14*) | 1.4 | 2.3 | -2.5 | *41* |
| Cs137 | *Fucus serratus* | 95 | 27 | 14 | 1.3 | 1.9 | -0.4 | *42* |
| | *Fucus serratus* | 34 | 29 | 30 | 1.2 | 1.8 | +1.4 | *43* |
| | *Fucus serratus* | 122 | 27 | 29 | 1.3 | 1.9 | -0.8 | *44* |
| | *Fucus serratus* | 98 | 22 | 30 | 1.4 | 2.3 | +0.7 | *45* |
| | *Fucus vesiculosus* | 87 | 30 | 30 | 1.3 | 2.1 | -1.2 | *46* |
| | *Fucus vesiculosus* | 87 | 26 | 30 | 1.4 | 2.1 | -0.6 | *47* |
| | *Patella sp* | 94 | 17 | 88 | 1.8 | 4.5 | +1.3 | *48* |
| | *Patella sp* | 33 | 11 | 30 | 1.3 | 1.8 | -1.3 | *49* |
| | *Patella sp* | 40 | 21 | 60 | 1.6 | 3.0 | +3.3 | *50* |
| | *Patella sp* | 52 | 18 | 50 | 1.5 | 2.4 | +6.0 | *51* |
| | *Patella sp* | 108 | 13 | 52 | 1.8 | 3.7 | +0.0 | *52* |
| | *Patella sp* | 86 | 11 | 55 | 1.7 | 3.1 | +5.6 | *53* |
| | *Mytilus edulis* | 67 | 12 | 30 | 1.8 | 3.8 | +5.8 | *54* |
| | *Mytilus edulis* | 51 | 20 | 40 | 2.4 | 5.0 | +15 | *55* |
| | *Mytilus edulis* | 63 | 8 | 72 | 1.7 | 2.8 | +5.0 | *56* |
| | (m)*Buccinum undatum* | 26 | 24 | 86 | 1.4 | 2.0 | -4.0 | *57* |
| | *Pecten maximus* | 39 | 20 | 21 | 1.8 | 4.5 | +7.5 | *58* |
| | *Pecten maximus* | 75 | 22 | 21 | 1.8 | 3.1 | +8.7 | *59* |
| | *Crassostrea gigas* | 36 | 10 | 46 | 1.5 | 2.1 | +0.0 | *60* |
| | *Cancer pagurus* | 86 | 23 | 60 | 1.6 | 2.7 | +4.0 | *61* |
| | *Cancer pagurus* | 103 | 23 | 60 | 1.4 | 2.0 | -0.4 | *62* |
| | *Cancer pagurus* | 14 | 27 | 30 | 1.6 | 2.8 | +10 | *63* |
| | *Homarus vulgaris* | 21 | 19 | 55 | 1.3 | 1.9 | +6.3 | *64* |
| | (f)Flat fish | 142 | 91 | 74 | 1.8 | 3.6 | -4.2 | *65* |
| | Flat fish | 98 | 85 | 45 | 1.2 | 2.9 | +8.6 | *66* |
| | (f)Round fish | 209 | 91 | 60 | 1.4 | 3.0 | +1.5 | *67* |
| | Round fish | 239 | 62 | 71 | 1.2 | 3.8 | +8.7 | *68* |
| | (f)*Labrus bergylta* | 22 | 86 | 75 | 1.6 | 2.6 | -3.3 | *69* |
| | (f)*Trisopterus luscus* | 9 | 54 | 59 | 1.5 | 2.2 | -2.5 | *70* |
| | *Trisopterus luscus* | 14 | 110 | 72 | 1.9 | 5.0 | +10 | *71* |
| | (f)*Scyliorhinus canicula* | 15 | 102 | 75 | 1.7 | 3.0 | +25 | *72* |
| | (f)*Scyliorhinus stellaris* | 16 | 160 | 75 | 1.9 | 3.0 | -20 | *73* |
| | (f)*Conger conger* | 19 | 69 | 55 | 1.4 | 2.2 | +1.7 | *74* |

Though they can be considered as non-soluble, some radionuclides were worth investigating anyway (see discussion section).

Table 2: CF and $tb_{1/2}$ values derived for each individual dataset (Rn, species) and scoring results of the model for non-soluble radionuclides. CF values are expressed in $L.Kg^{-1}$ and $tb_{1/2}$ values in day.

| **Rn** | (Grp)**biota** | **nb Obs** | **CF** | **$tb_{1/2}$** | **Rmean** | **R95** | **Rc50(%)** | **dataset #** |
|---|---|---|---|---|---|---|---|---|
| Mn54 | *Fucus serratus* | 75 | 2 69 | 122 | 1.7 | 3.2 | +0.8 | *75* |
| | *Fucus vesiculosus* | 44 | 1 600 | (120) | 2.4 | 6.0 | -4.0 | *76* |
| | *Pecten maximus* | 24 | 1 300 | 107 | 1.7 | 3.3 | +0.0 | *77* |
| | *Pecten maximus* | 38 | 1 300 | (120) | 1.9 | 3.6 | +0.0 | *78* |
| | *Cancer pagurus* | 13 | 1 800 | 240 | 2.3 | 5.0 | +5.0 | *79* |

| | | | | | | | | |
|---|---|---|---|---|---|---|---|---|
| Co60 (dist./ outlet, Km) | *Fucus serratus* (6 Km) | 89 | 1556 | 128 | 1.4 | 2.0 | -1.3 | *80* |
| | *Fucus serratus* (6 Km) | 35 | 2183 | (14) | 1.6 | 2.7 | +3.8 | *81* |
| | *Fucus serratus* (12 km) | 113 | 2261 | 95 | 1.4 | 2.3 | +4.5 | *82* |
| | *Fucus serratus* (45 Km) | 104 | 536 | (120) | 1.4 | 2.7 | -0.9 | *83* |
| | *Fucus vesiculosus* (12 km) | 88 | 1683 | 95 | 1.4 | 1.9 | +0.9 | *84* |
| | *Fucus vesiculosus* (45 Km) | 89 | 434 | (120) | 1.4 | 2.4 | -1.7 | *85* |
| | *Patella sp* (6 Km) | 129 | 619 | 30 | 1.7 | 3.2 | -0.6 | *86* |
| | *Patella sp* (6 Km) | 65 | 450 | 60 | 1.4 | 2.0 | -2.8 | *87* |
| | *Patella sp* (12 Km) | 92 | 435 | 30 | 1.6 | 2.8 | +1.0 | *88* |
| | *Patella sp* (45 Km) | 128 | 158 | 60 | 2.1 | 5.0 | +5.5 | *89* |
| | *Patella sp* (15 Km) | 126 | 406 | 60 | 1.9 | 4.5 | -0.8 | *90* |
| | *Patella sp* (42 Km) | 125 | 299 | 60 | 1.7 | 3.4 | +5.4 | *91* |
| | *Buccinum undatum* (18 Km) | 114 | 714 | 120 | 2.2 | 3.4 | -3.6 | *92* |
| | *Mytilus edulis* (18 Km) | 53 | 430 | 60 | 1.8 | 3.7 | -1.3 | *93* |
| | *Mytilus edulis* (34 Km) | 67 | 225 | 60 | 1.9 | 3.2 | -17 | *94* |
| | *Mytilus edulis* (82 Km) | 180 | 57 | 60 | 1.8 | 6.0 | +0.0 | *95* |
| | *Crassostrea gigas* (82 Km) | 151 | 89 | 140 | 2.0 | 4.5 | +2.9 | *96* |
| | *Pecten maximus* (18 Km) | 11 | 571 | 140 | 2.9 | 6.0 | +2.5 | *97* |
| | *Pecten maximus* (34 Km) | 98 | 677 | 140 | 1.5 | 2.6 | +2.0 | *98* |
| | *Cancer pagurus* (18 Km) | 273 | 492 | 30 | 1.7 | 2.7 | +2.8 | *99* |
| | *Cancer pagurus* (2 Km) | 17 | 1848 | 30 | 2.0 | 6.0 | -1.7 | *100* |
| | *Cancer pagurus* (34 Km) | 221 | 889 | 30 | 1.8 | 3.9 | +0.3 | *101* |
| | *Homarus vulgaris* (42 Km) | 18 | 621 | 30 | 2.7 | 3.8 | +5.0 | *102* |
| | Flat fish (misc. sp.) (18 km) | 40 | 138 | 60 | 1.8 | 3.5 | +3.3 | *103* |
| | Flat fish (34 km) | 28 | 36 | 60 | 3.0 | 6.0 | +0.0 | *104* |
| | Round fish (misc. sp.) (18 km) | 104 | 90 | 60 | 2.2 | 5.0 | +2.2 | *105* |
| | Round fish (2 km) | 48 | 133 | 60 | 3.0 | 6.0 | +0.0 | *106* |
| | Round fish (34 km) | 49 | 32 | 60 | 3.0 | 6.0 | +2.5 | *107* |
| Zn65 | *Fucus serratus* | 39 | 8579 | 95 | 1.6 | 4.5 | -1.7 | *108* |
| | *Patella sp* | 52 | 9473 | 53 | 1.7 | 3.1 | +4.0 | *109* |
| | *Patella sp* | 29 | 6869 | 38 | 2.5 | 5.0 | +7.5 | *110* |
| | *Patella sp* | 17 | 3097 | (60) | 1.3 | 1.9 | +5.0 | *111* |
| | *Crassostrea gigas* | 53 | 9903 | (60) | 1.7 | 3.4 | -9.0 | *112* |
| | *Cancer pagurus* | 59 | 13953 | (60) | 1.9 | 4.0 | -0.8 | *113* |
| Ru106 | *Fucus serratus* | 63 | 93 | 60 | 1.8 | 2.4 | -0.8 | *114* |
| | *Fucus serratus* | 99 | 89 | 25 | 1.6 | 3.0 | +3.6 | *115* |
| | *Fucus serratus* | 81 | 21 | 58 | 1.7 | 3.4 | +6.4 | *116* |
| | *Fucus vesiculosus* | 53 | 53 | 41 | 1.6 | 3.4 | +1.3 | *117* |
| | *Fucus vesiculosus* | 43 | 13 | 30 | 1.7 | 3.3 | -5.0 | *118* |
| | *Patella sp* | 122 | 142 | 53 | 1.8 | 5.0 | +3.1 | *119* |
| | *Patella sp* | 42 | 75 | 60 | 1.9 | 3.7 | +0.0 | *120* |
| | *Patella sp* | 110 | 120 | 60 | 2.5 | 5.0 | +0.0 | *121* |
| | *Patella sp* | 14 | 63 | 158 | 1.7 | 4.5 | +6.7 | *122* |
| | *Patella sp* | 124 | 98 | 92 | 1.8 | 3.7 | +8.6 | *123* |
| | *Patella sp* | 59 | 14 | 60 | 1.7 | 3.8 | +1.3 | *124* |
| | *Patella sp* | 111 | 78 | 60 | 1.7 | 3.9 | -1.9 | *125* |
| | *Mytilus edulis* | 12 | 81 | 40 | 1.6 | 2.5 | +20 | *126* |

| | | | | | | | |
|---|---|---|---|---|---|---|---|
| *Mytilus edulis* | 160 | 36 | 77 | 2.0 | 4.5 | +14 | *127* |
| *Buccinum undatum* | 71 | 340 | 60 | 2.1 | 6.0 | -3.0 | *128* |
| *Buccinum undatum* | 10 | 74 | 60 | 1.8 | 3.7 | +0.0 | *129* |
| *Pecten maximus* | 43 | 249 | 85 | 1.7 | 3.0 | -1.0 | *130* |
| *Pecten maximus* | 84 | 148 | 60 | 1.7 | 3.4 | -1.3 | *131* |
| *Pecten maximus* | 11 | 375 | 60 | 2.8 | 6.0 | -5.0 | *132* |
| *Crassostrea gigas* | 82 | 24 | 60 | 1.7 | 3.5 | +5.0 | *133* |
| *Cancer pagurus* | 15 | 175 | 14 | 1.6 | 2.6 | +11 | *134* |
| *Cancer pagurus* | 120 | 85 | 14 | 2.2 | 5.5 | +5.0 | *135* |
| *Cancer pagurus* | 8 | 2 | 14 | 1.4 | 2.2 | +0.0 | *136* |

### 3.3 Apparent CF change with distance to the source of input

In the case of iodine-129 in brown seaweed, though the CF is supposed to be independent of location, a clear apparent decrease of estimated CF values with distance from the source of input was observed. This apparent decrease with distance is addressed in the Discussion section.

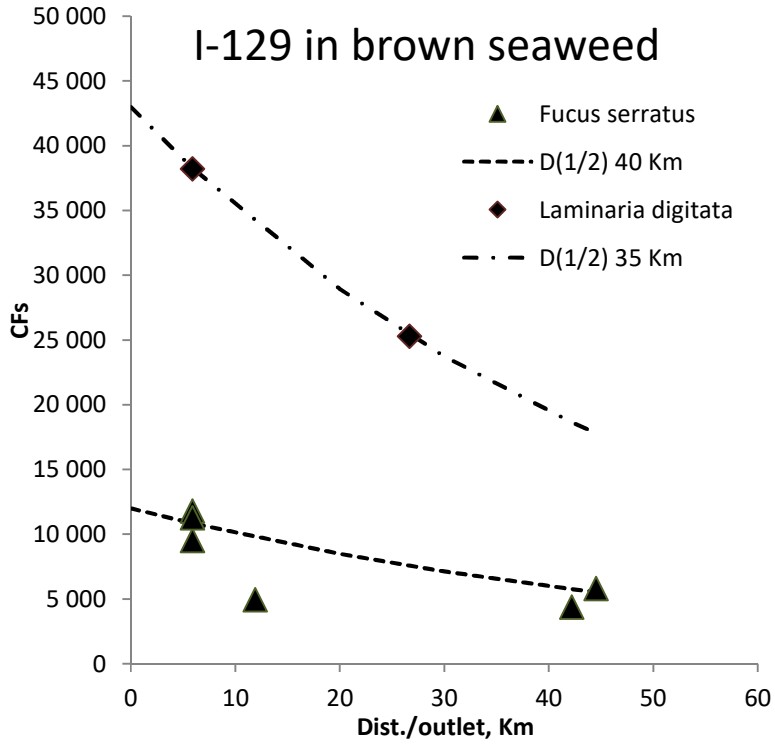


Figure 5: Apparent changes in I129 CF values in brown macroalgae (symbols) with distance from the outlet of the RP. Dashed lines correspond to exponential decrease functions (that should not be extended further, see Discussion).

In the case of cobalt-60, though the reasons may be different from iodine-129, a clear apparent decrease of estimated CF values with distance from the source of input was also observed. Likewise Iodine-129 in seaweed, this apparent decrease is addressed in the Discussion section.

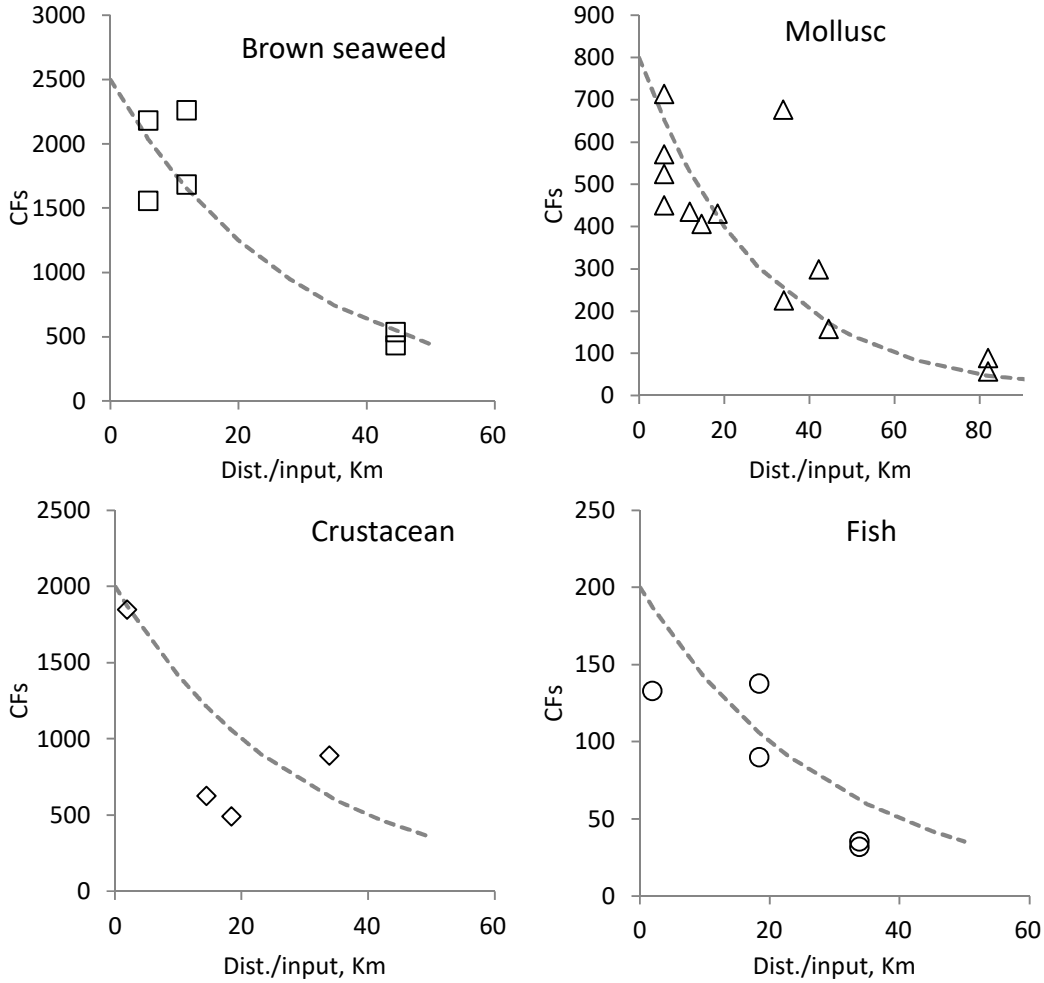


Figure 6: Apparent changes in Co60 CF values (symbols) in the four biota groups (macroalgae, mollusk, crustacean and fish) with distance from the outlet of the RP. Dashed lines correspond to exponential decrease functions (that should not be extended further, see Discussion) with a $D_{1/2}$ = 20 Km.

### 3.4 Recommendations by biota group

Table 3: CF and $tb_{1/2}$ values derived from merged datasets by biological groups and scoring results of the model for soluble radionuclides. * IAEA TRS-422, (2004).

| **Rn** | **biota group** *(IAEA CF*)* | **nb Obs** | **CF** | **tb1/2(d)** | **Rmean** | **R95** | **Rc50(%)** |
|---|---|---|---|---|---|---|---|
| H, biota | Macroalgae *(1)* | 106 | 1.0 | 0.3 | 1.5 | 2.5 | +22.9 |
| water | Mollusc *(1)* | 37 | 1.0 | 0.3 | 1.5 | 2.7 | +11.7 |
| H, organ. | Macroalgae *(1)* | 115 | 1.0 | 120 | 1.3 | 1.8 | +12.3 |
| bound | Mollusc *(1)* | 40 | 1.0 | 150 | 1.2 | 1.5 | +20.9 |
| C | Macroalgae *(10 000)* | 69 | 3 500 | 45 | 1.1 | 1.3 | -0.8 |
| | Mollusc *(20 000)* | 98 | 3 800 | 90 | 1.1 | 1.3 | -0.6 |
| | Crustacean *(20 000)* | 13 | 4 200 | 45 | 1.1 | 1.4 | +1.7 |
| | Fish *(20 000)* | 8 | 4 600 | (120) | 1.1 | 1.2 | +0.0 |
| Sb | Macroalgae *(20)* | 192 | 11 | 45 | 1.5 | 2.7 | +6.3 |
| | Mollusc *(300)* | 346 | 8 | 45 | 1.9 | 4.5 | -2.6 |
| | Crustacean *(300)* | 93 | 10 | 120 | 1.7 | 2.9 | +8.8 |

| | | | | | | | |
|---|---|---|---|---|---|---|---|
| I** | Macroalgae *(10 000)* | 199 | 20 000 | 14 | (*2.3* | *5.5* | *+46*) |
| | Wrack | 154 | 12 000 | 20 | 1.5 | 2.8 | +4.7 |
| | Kelp | 45 | 43 000 | 14 | 1.6 | 2.8 | +1.7 |
| Cs | Macroalgae *(50)* | 523 | 28 | 30 | 1.4 | 2.2 | +3.8 |
| | Mollusc *(60)* | 737 | 16 | 60 | 2.0 | 4.5 | +3.0 |
| | Crustacean *(50)* | 224 | 22 | 60 | 1.5 | 2.3 | +7.7 |
| | Fish *(100)* | 783 | 75 | 75 | 1.8 | 3.7 | +7.3 |

For I129(**), an arbitrary exponential decrease in bioavailability with distance (half-distance of 40Km) was implemented to account for the apparent change in CF value with distance from the source of input (see section 3.3). The scoring results depended on the proportion of wrack and kelp species for which the macroalgae CF value of 20 000 yielded over- or under-estimation, respectively.

Table 4: CF and $tb_{1/2}$ values derived from merged datasets by biological groups and scoring results of the model for non-soluble radionuclides. * IAEA TRS-422, (2004).

| **Rn** | **biota group** *(IAEA CF*)* | **nb Obs** | **CF** | **tb1/2(d)** | **Rmean** | **R95** | **Rc50(%)** |
|---|---|---|---|---|---|---|---|
| Mn | Macroalgae *(6 000)* | 143 | 2 200 | 120 | 3.7 | 9.4 | -1.0 |
| | Mollusc *(50 000)* | 63 | 1 400 | 100 | 1.9 | 3.7 | +3.8 |
| | Crustacean *(5 000)* | 15 | 1 800 | 240 | 2.3 | 5.0 | +5.0 |
| Co*** | Macroalgae (6 000) | 518 | 2 400 | 120 | 1.5 | 2.5 | -0.6 |
| | Mollusc *(20 000)* | 1339 | 900 | 90 | 2.3 | 5.5 | -1.9 |
| | Crustacean *(7 000)* | 529 | 1 300 | 30 | 2.3 | 5.0 | +2.8 |
| | Fish *(700)* | 269 | 200 | 60 | 2.5 | 6.0 | +6.1 |
| Zn | Macroalgae *(2 000)* | 39 | 8 500 | 90 | 1.6 | 4.5 | -1.7 |
| | Mollusc *(80 000)* | 148 | 8 500 | 60 | 2.0 | 4.0 | +0.0 |
| | Crustacean *(300 000)* | 59 | 14 000 | 60 | 1.9 | 4.0 | +7.5 |
| Ru | Macroalgae *(2 000)* | 339 | 60 | 45 | 2.7 | 6.0 | +20 |
| | Mollusc *(500)* | 1055 | 100 | 60 | 3.1 | 6.0 | +12 |
| | Crustacean *(100)* | 143 | 90 | 14 | 5.2 | 6.0 | +6.3 |

For Co60 (***), an arbitrary exponential decrease in bioavailability with distance (half-distance of 20 Km) was implemented to account for the apparent change in CF value with distance from the source of input (see section 3.3).

### 3.5 Overall reliability scoring of the model

An overall scoring of the modelling performances was finally performed by merging all R and Rc values from all datasets (radionuclide/species/location). A nested donut chart visually indicated the relative weights of radionuclides and biota groups in this overall scoring. Histograms and cumulative percentages of R and Rc provided a distribution analysis of these scores. Altogether, the 136 datasets included 8241 individual observation data compared to their corresponding values calculated by the model (Figure 7). The R and Rc values were calculated with 1- optimal transfer parameters derived from each individual dataset fitting (Section 3.2) and 2- transfer parameters values recommended for biota groups (Section 3.4). In the first case (optimal individual datasets fitting), Rmean = 1.71, R50 (median) = 1.41, R95 < 3.4 and Rc50 = +5.5%. When using transfer parameters values recommended for biota groups, a slight decrease in the modelling performance was expectedly observed with Rmean = 2.13, R50 = 1.54, R95 < 5.0 and Rc50 = +9.5%. In both cases, the positive values of Rc50

meant a slight overestimation by the model which guaranteed conservative results as regards radioprotection. Outlier R values greater than 5 accounted for less than 5% (4.64%) of observations, they distributed evenly outside the [-4..4] range of Rc.

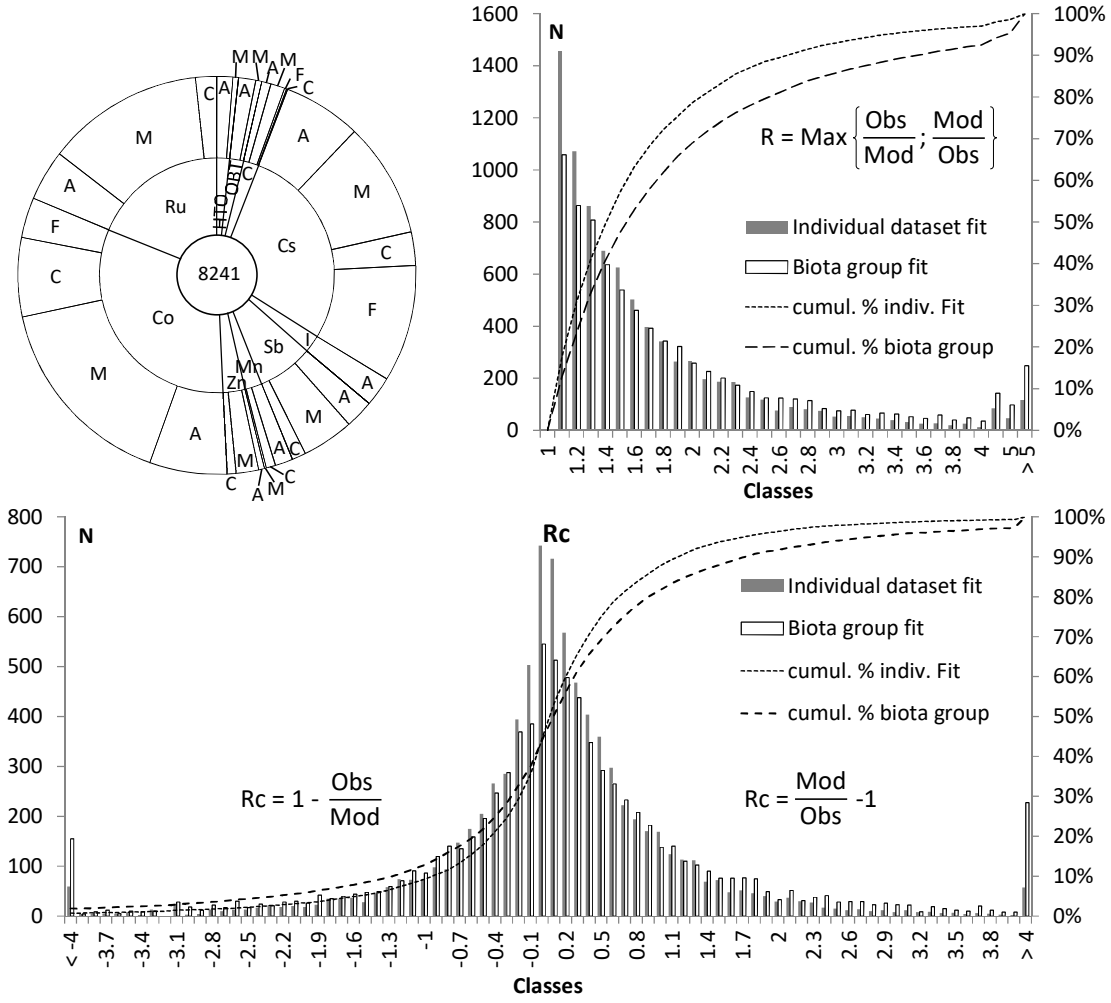


Figure 7: Summary of overall scoring of the model performances based on the distributions of all residual R and Rc values (see section 2.3.2). Top-left: Donut graph showing the relative contributions of biota groups (Outer: A macroalgae; M mollusk; C crustacean; F fish) per radionuclides (inner) to the total 8241 observation data. Top-Right: Histogram and cumulative percentage of R values. Bottom: Histogram and cumulative percentage of Rc values. R and Rc scored the model with the individual datasets or biota groups optimal parameters for comparison (see text section 3.5).

## 4 Discussion

### 4.1 Estimation of the transfer parameters values

The values were selected using the following procedures. A first "brutal" residual minimization as described in section 2.3.2 was carried out as a first step to estimate CF and $tb_{1/2}$ values. The estimation of CF values was quite robust because a vertical shift of the model directly resulted from changes in the value of CF. Minimizing the residual mathematically constrained a good match of the general level of the model signal to the observation dataset. The CF value was relevant but in some cases this yielded a very long $tb_{1/2}$ value (>> 100 y). It resulted in a flat smoothed calculated signal across scattered observation data in the biota and was not realistic. As a second step, a focus was made on parts of the dataset where the signal in seawater displayed large magnitude changes because in such case, the changes in biota are very sensitive to the value of $tb_{1/2}$. For example, a large

and long lasting increase/decrease in biota concomitant to that in seawater was focused on to constraint the estimation of $tb_{1/2}$ value. This second step was performed visually and rounded values of $tb_{1/2}$ were taken. More accurate values would not make sense because of high data scattering as illustrated in the examples in section 3.1. Once those constrained values of $tb_{1/2}$ were chosen and fixed, the CF values were further adjusted by minimizing the residual. Finally, there were some cases where the number of data was small or the time intervals between observations were too long to estimate $tb_{1/2}$ accurately and the value was arbitrarily set on the basis of similar dataset analysis (same radionuclide and biota). Because of the data variety and scattering as well as uncertainties (with mobile species for example), there was no universal calculation method to be used systematically and blindly to derive the parameters values in every cases. Some "fitting by eye" was obviously necessary to drive the estimation, especially $tb_{1/2}$. For this reason, it was essential to provide some scoring of the model's reliability which supported the relevancy of the parameters values proposed in this paper. These were the purposes of R and Rc residual calculations.

### 4.2 Performance of the transfer model

The R and Rc residuals between the model and observations described in section 3.1 served two objectives. R was used as a residual minimizing criterion ($R \geq 1$; 1 meant perfect match) and Rc median (Rc50 in %) was kept as close to 0 as possible (R=0 meant perfect match). When optimal R yielded an Rc50 value below -10%, CF was raised (which could slightly increase R) to prevent too much under-estimation by the model because this would potentially yield non-conservative results. A sensitivity analysis of the model performance on the derived values of $tb_{1/2}$ was carried out by using R and Rc values as shown at the end of section 3.1. It illustrated how both R and Rc residual metrics combined to yield optimal transfer parameters values. The second objective of R and Rc was to document the reliability of the model's prediction. R indicated the mismatch ratio between the model and the observations (lower or greater), it was reported as its average (Rmean) and its value for 95% of observation data (R95). The R95 value provided an estimate of the overall reliability of the model. For soluble radionuclides, R95 was found up to 5 but usually lower than 3. This scoring of 3 is outstanding because it meant that for almost all (95%) individual observation data, the model estimations mismatched by less than a factor 3. It should be reminded that the only radionuclide input data in the model were the discharges from the reprocessing plant. The radionuclide concentrations in seawater at any location and date in the English Channel were calculated by the hydrodynamic model MARS-2D (Bailly du Bois et al., 2012, 2020). Then the concentrations in biota were derived from the concentrations in seawater by the dynamic transfer model (Fiévet et al., 2003) using the proposed parameters CF and $tb_{1/2}$. All sources of variability and uncertainties included in this calculation chain typically resulted in only a factor 3 mismatch. Except for Mn in macroalgae where it reached 9.5, R95 stayed lower or equal 6. When merging residual R and Rc values from all 8241 observation data and their corresponding values predicted by the model with CF and $tb_{1/2}$ parameters recommended for biota groups, the mismatch stayed lower than a factor of 5 (R95) with a median (R50) of 1.54 (Section 3.5). These score values supported the performance of the overall modelling of dispersion in seawater of radionuclide discharges by the RP and their transfer to biota with only the discharges data as the input.

### 4.3 Non-soluble radionuclides

Although still acceptable, the performances of the model were obviously degraded when dealing with non-soluble radionuclides. By definition non-soluble radionuclides disappear from the water column more or less rapidly by sedimentation which potentially influences their bioavailability. Non-soluble radionuclides associate with particulate material and the smaller the particles, the higher their affinity. Previous radionuclide discharges trapped in sediment may return to the water column by resuspension. But since the amounts of most liquid radioactive discharges from the RP has

substantially declined since the 80' (https://www.orano.group; Fiévet et al., 2020), the influence of radionuclide potentially remobilized from the sediment compartment increases relatively with respect to that of recent discharges. Moreover, the isotopic signature of remobilized discharges may be different from that of recent ones. The contribution of this secondary sources of radionuclides occurs through a partial return to the water column as well as contamination by particulate material sticking to protective mucus or in the digestive tract (if present) by marine species. The influence of this secondary source of radionuclides results in a potential disconnection of the levels of non-soluble radionuclides in biota time series measurements from concomitant discharges. In recent observations (mid 2010'), the levels of these radionuclides in biota could not be quantitatively related to concomitant discharges from the RP (Fiévet *et al.*, 2020). Interestingly, they appeared to follow the seasonal cycle of seawater mineral suspended matter in the English Channel (Gohin, 2010; Rivier, 2013). In our previous review on the dispersion and transfer to biota of radioactive discharges from the RP in the English Channel, we identified Co60 and Ru106 in this category (Fiévet *et al.*, 2020). In this study, radionuclides concentrations in seawater were calculated by the hydrodynamic model (as if they were soluble). For non-soluble radionuclides, the resulting calculated concentrations were thus likely to be overestimated. The further from the source of input, the bigger the discrepancy between the real concentrations in seawater and those calculated by the MARS-2D model. So, why address non-soluble radionuclides in this study? Datasets #75 to #136 included rich time-series measurements for Mn54, Co60, Zn65 and Ru106, many of which starting in the 80'. By this time radioactive discharges were relatively higher so the contribution of the sediment compartment was not as dominant as in the 2010' (Fiévet *et al.*, 2020). Even though the contribution of suspended material was sometimes visible by seasonal oscillations around the trend of the signal, the time series spanned over the general decline in the discharges. As explained above (section 4.1), a long lasting negative trend of the signal in seawater was particularly well fit to estimate $tb_{1/2}$ in biota. So these datasets for those non-soluble radionuclides were tentatively investigated and scoring the model performance through R and Rc relative residual values assessed their relevancy. For individual datasets (#75 to #136) Rmean eventually exceeded 2.0 whilst R95 often exceeded 3.0, up to 6.0. For biota groups, Rmean occasionally exceeded 3.0 with R95 up to 9.4. Though these performance scores were not as good as for soluble radionuclides, the reliability of the modelling is still noteworthy. It should be repeated that the performance scoring covers modelling imperfections all the way from the amounts of radionuclide discharges, the calculation of seawater activities, down to concentrations in biota.

### 4.4 Apparent decrease in CF values with distance from the outlet of the RP

In two particular cases, a decrease in bioavailability with distance from the outlet of the RP was obvious and was tentatively taken into account. In the case of I129, fitting the observational data time series of individual datasets #34 to #41 with the model yielded an apparent decrease in CF with distance from the outlet (this was the reason why distances were added in the table for this radionuclide). However there was no reason why I129 CF should depend on the location of the seaweed. I129 is expectedly released by the RP as soluble to mix with natural seawater stable iodine in order to optimize isotopic dilution. In seawater, dissolved iodine is present as iodate ($IO_3^-$) and iodide ($I^-$). Although iodate is the spontaneous chemical state of dissolved iodine in seawater because of pH and redox potential, both chemical forms are present in various proportions (see Wong, 1991; Hou *et al.*, 2007; Carpenter, 2013, for reviews). For thermodynamic reasons, reduction of iodate into iodide is not spontaneous in natural seawater and the mechanisms of conversion between iodine species is still not clear (Hou *et al.*, 2007). However this reaction between iodate and iodide takes some time to reach a balance, which was estimated around two weeks (Carpenter, pers. Comm.). The speciation of dissolved iodine in seawater raises 3 questions: 1- What is the chemical form of I-

129 at the outlet of the RP? 2- Which chemical form of iodine is bioavailable for brown seaweed? 3- How does the chemical speciation of I129 evolve with time and distance of dispersion from the source of input? The chemical form of liquid radioactive iodine released by nuclear facilities is not yet available but it is thought to be as iodide (Hou *et al.*, 2013; Zhang and Hou, 2013). If we assume that I129 is released in the form of iodide, once introduced in seawater, I129 undergoes the slow conversion process between iodide and iodate. As far as we know, iodine uptake by brown seaweed is mediated by enzymes from the family of vanadate-haloperoxydases (Küpper *et al.*, 1998) whose substrate are halogens in the form of halide (Coplas *et al.*, 1996). An iodine-specific iodoperoxidase has been identified in *Laminaria digitata* (Colin *et al.*, 2005) and, as a member of the enzyme family, its substrate is assumed to be iodide. These answers to the first two questions still require confirmation and further clarification. However, on the basis of these provisional and partial answers, it can be proposed that bioavailability of I129 for brown seaweed may disconnect from the concentrations in seawater calculated by the hydrodynamic model. If I129 is released as iodide-129, it can be assumed to be fully available for seaweed. But as iodide-129 slowly converts into iodate-129, it becomes unavailable for seaweed. As distance (and time of dispersion) from the source of input increases, the gap between I129 bioavailable for seaweed and I129 activity calculated in seawater by the hydrodynamic model increases. This phenomenon evolves until the isotopic ratios I129/I127 in seawater iodate and iodide are identical. But the magnitude of the discrepancy depends on the proportions between seawater iodate and iodide. The chemical speciation of I129 in seawater and its changes obviously require further investigation. But so far, although I129 is considered as a soluble radionuclide, the apparent decrease of its CF derived from the observed time series measurements in brown seaweed with distance from the outlet of the RP was likely to result from a decrease of seawater I129 bioavailability compared to its activity calculated by the MARS-2D model. Over-estimating seawater bioavailable concentrations mathematically resulted in under-estimating CF values and it explained the apparent reduction of CF with distance. This proposed explanation for I129 CF decrease with distance from the RP is still speculative at this point. Furthermore, the geographical area of available datasets is limited and long distance data are obviously required to further characterize the phenomenon. Nevertheless, the aim of this study was to provide recommendation for transfer parameter values so two values of CF were tentatively proposed for wrack and kelp. Up to a distance of 50 Km, a correction of seawater concentrations was implemented as a simple exponential decrease relationship with distance to roughly account for the observed decreases of CF values with distance from the RP. The relationship were derived from the graphical representation of CF *vs* distance and Log[CF] vs Dist. linear regression analysis. CF values were back extrapolated to distance 0 which yielded 12 000 and 43 000 for wrack and kelp respectively. A value of 20 000 was proposed for brown macroalgae. The half distance reduction of concentrations ($D_{1/2}$) derived from the Log[CF] vs Dist. linear regression analysis yielded similar values of 40 and 35 Km for wrack and kelp, respectively. The poor number of data points could not justify an accurate value so $D_{1/2}$ was rounded to 40 Km as a recommendation for brown seaweed. Moreover, it must be emphasized that the validity of the exponential decrease was strictly limited to the range of distances up to 50 Km where the actual observational datasets (#34 to #41) were available. As explained above, the decrease in I129 bioavailability is expected to level off when the isotopic ratio I129/I127 is identical in iodide and iodate. The distance (and time) to reach this steady state depends on the ratio between iodide and iodate but I129 bioavailability is not expected to tend to zero as implemented by an exponential decrease. Because we lacked long distance observational dataset, we could not estimate any steady state value and proposed a more realistic decreasing function to account for the phenomenon beyond 50 Km. Since the proposed CF values were back extrapolated to zero distance, this meant that all I129 was assumed to be as iodide or at least bioavailable for brown algae. At a longer distance, if we assume that iodide and iodate are in steady state with an even partition of 1/1

and that iodate is no more bioavailable, this means that CF values should be divided by 2 because only half of I129 remains as iodide. I129 transfer to brown seaweed clearly requires to be thoroughly explored, regarding iodine chemical speciation and at longer distances.

In the case of Co60, fitting the observational data time series of individual datasets #80 to #107 with the model yielded an apparent decrease in CF with distance from the outlet (likewise I129, the distances were added in the table for this radionuclide). However there is no reason why Co60 CF should depend on the location of the biota. Though it has a half-life of 5.27 years, Co60 was continuously present in the discharges from the plant and it is known to be mainly released as particulate material (Gaudaire, 1996). It is thus expected to sediment with particulate material, to disappear from the water column and the further the distance (and thus time of dispersion) the lower the levels. This phenomenon being not implemented in the calculations by the hydrodynamic model, seawater concentrations were over-estimated with respect to real values. Over-estimating seawater concentrations for non-conservative radionuclides mathematically resulted in underestimating CF values and it explained the apparent reduction of Co-60 CF with distance. This reduction was clearly pointed out from seawater measurements in Bailly du Bois and Guégueniat (1999) with an average loss of 96% of the dissolved Co-60 at the scale of the English Channel. The overall phenomenon includes many complex processes as interactions between Co60 and suspended matter, particle size, sedimentation of particulate material, sediment resuspension and transport, potential redissolution of radionuclides from sediment material (return to the water column) and interactions with biota (adsorbed/ingested). A hydro-sedimentary model accounting realistically for transport of thin particles mixed with the coarser ones is expected to much better represent the behavior of Co-60 (Rivier *et al.*, 2017). Likewise I129, a simple exponential decrease relationship was obviously a rough implementation and very few scattered data points were available to account for the decline of Co60 concentration in seawater with distance from the RP. Moreover in the absence of long distance observational time series measurement in biota, the validity of the relationship is strictly limited to the area of available datasets around the North end of the Cotentin peninsula. The exponential decrease relationships were estimated from the biota groups' scattergrams of Log[CF] vs Dist. by linear regression. Recommended CF values were back extrapolated at distance 0 for each biota group and an average $D_{1/2}$ value of 19.3 Km was obtained for all four groups. Because of the very simple mathematical implementation of such a complex phenomenon and the intrinsic uncertainty on this $D_{1/2}$ value, it was considered that 3 significant digits would not make sense. In the context of recommendations of generic parameters for radioprotection modelling purpose, it was considered that rounding $D_{1/2}$ to 20 Km was reasonable enough until a more scientific mastering of non-soluble radionuclides transport in the English Channel is available. Finally, although Co60 is an example of non-soluble radionuclide for which waterborne transport and transfer modelling from the discharges to the biota should be taken with caution, the scoring performances obtained in this study remained acceptable in the restricted geographical area.

For both I129 and Co60, two arguments could be proposed to support this estimation of the values of $D_{1/2}$ used in the restricted area: 1 - The estimation of CF values was quite robust as explained in section 4.1. Though the data are scattered on graphs CF vs Dist., the CF value à Dist. = 0 and the slope using a rounded value of $D_{1/2}$ appeared visually realistic (Figure 5 and Figure 6). 2- Since $D_{1/2}$ was designed to implement the decrease in concentration of I129 (as bioavailable for brown seaweed) and Co60 in seawater with distance, it should not depend on the biota. For Co60, the same value of $D_{1/2}$ = 20 Km could be used consistently for all biota group, whatever the CF ranges. Interestingly, Co60 concentrations in biota reported in our recent review around the Channel Islands confirmed that this radionuclide is detected in seaweed and limpet only at short distance from the outlet of the RP (Fiévet *et al.*, 2020). For I129, $D_{1/2}$ distances of 35 Km and 40 Km for kelp and wrack were

proposed with a satisfactorily scoring of the model performances. However though wrack and kelp $D_{1/2}$ values were close enough, the CF values for those two types of brown algae were clearly distinct and using and intermediate CF value degraded the performances of the model.

### 4.5 Comparison with CF and $tb_{1/2}$ values from the literature

The CF values recommended for steady state situations from IAEA TRS 422 (IAEA, 2004) were reported in Table 3 and Table 4 as an indication for comparison with the CF values derived in our study. TRS 422 CF values were revised in TRS 479 (IAEA 2014) where updated values were reported as arithmetic and geometric means, as well as min-max ranges. It should be reminded that those values (or ranges) were recommended in the context of radioprotection so they are assumed to be rather conservative. There is an agreement for tritium, which is consistent since the element does not bioaccumulate in living matter and tritium is discharged in seawater as HTO by the RP (Fiévet *et al.*, 2013). For the majority of other radionuclides investigated here, our recommended CF values were lower than those from IAEA TRS 422. For Carbon, our measurement data were obtained in a context where C14 was discharged by the RP as dissolved inorganic carbon (DIC) (Douville *et al.*, 2004) and on the basis of the element content in dry organic matter (40-50%), our values for C14 are consistent with the CF of the stable element and with our previous study (Fiévet *et al.*, 2006). This is in agreement with the revision of C14 CF values in TRS 479 (IAEA, 2014). For Iodine, our CF value in wrack was consistent with the value of 10 000 in TRS 422 and the outstanding capacity of kelp to concentrate this element is a particular case. We raised the issue of I129 chemical speciation in the marine environment of the RP outlet and we outlined the limited validity of our recommended FC value within 50 Km from the RP. Although our FC value in wrack was consistent with the value reported by Gómez-Guzmán et al., (2014) in Kattegat, the fate of I129 released by the ORANO La Hague RP obviously needs further investigation. For Antimony, our derived CF are below those reported in TRS 479, this was surprising since the latter were mainly derived from data from IRSN in the English Channel. This illustrated how the data processing method to derive average CF values was crucial. For Cs, there were a lot of measurement data available (Figure 7, Donut graph), our CF values were below those from TRS 422 but a closer look at the most recent updated CF values from TRS 479 showed a good agreement. For Mn and Co, our recommended CF values were below those from TRS 422 but they were still in the wide ranges reported in TRS 479. For Ru and Zn our recommended CF values were below the ranges of TRS 479. For those four last radionuclides, we expected to face difficulties when estimating seawater concentration assuming they spread like soluble substances. Concentrations in the water may have been overestimated which yielded lower CF values, so our results should be considered cautiously.

Whatever the values of CF, either derived in this study or those expectedly conservative from TRS 422 and TRS 479, the biological half-life values were obviously the main originality of our work. Our recommended $tb_{1/2}$ values were designed for operational modelling. As explained in the introduction, they implement all environmental processes responsible for depuration of the radionuclides from marine species populations. Comparing our values with those from the literature was challenging, certainly the reason why no recommendation exists so far. For each radionuclide and biota group, $tb_{1/2}$ values gathered in the reviews by Gomes *et al.*, (1991) and more recently by Beresford *et al.*, (2015) spanned over very wide ranges. Several radionuclides investigated here were not covered, (H3, C14) or very little (Sb125). The majority of the $tb_{1/2}$ were determined in laboratory experimental conditions. Nevertheless, we can outline a good agreement for Iodine, though different isotopes, a good agreement for Cs, though no data for crustacean. For Mn, our values in mollusk appear much longer than determined in laboratory experiments. For Co, there was no data available for macroalgae but there was a good agreement for other biota groups. For Zn and Ru, our $tb_{1/2}$ values were in the wide ranges of the values gathered in the review by Beresford *et al.*, (2015).

### 4.6 Validity of the recommended dynamic transfer parameters values as regards the geographical area

The performances of the model could have been expected to be better for sessile species (i.e. wrack, kelp, limpet, mussel, oyster) compared to mobile ones (i.e. scallops, crabs, lobsters, fish) because uncertainty on the location of the animal directly reflected on uncertainty on the activity in seawater (example: Figure 3). However, except maybe for Co60 in fish, no clear increase in the values of Rmean and R95 were observed for mobile species. It should be outlined that the English Channel is a relatively small shallow macrotidal Sea between France and the United-Kingdom, entirely located on the continental shelf, where mobile local species collected for monitoring are probably confined. The uncertainty on their location was reflected in the distribution of the residual and did not challenge the data processing strategy. This suggests that the arbitrary averaging area of 3.5 km x 3.5 km seawater modelling data for mobile species was a reasonable guess. Migrating species spending only part of their time in the area may require some adaptation of this modelling like what we proposed in the context of FDNPP accident (Fiévet *et al.*, 2017).

For soluble radionuclides H3 (as HTO and as OBT), C14, Sb125 and Cs137, there are no reason why the recommended values of CF and $tb_{1/2}$ proposed here should not be used elsewhere in the marine environment, though some issues in very different latitudes cannot be ruled out (intertropical, Arctic and Antarctic marine environment). For I129, its bioavailability for seaweed is likely to be influenced by its chemical speciation. An empirical exponential decrease relationship appeared to fit the observation data and was implemented within 50 Km from the source of input. At a longer distance, depending on the proportion of I129 which remains bioavailable for brown seaweed, the CF values should be scaled down accordingly. Nevertheless, the CF value of 10 000 reported by Gómez-Guzmán *et al.*, (2014) in *Fucus* from Kattegat (Denmark), far away downstream the outlet of the RP (no other source of I129 to our knowledge), was consistent with our recommended value. Investigating the fate of the chemical speciation of I129 released by the RP thoroughly is a prerequisite before we can consolidate the validity of our transfer modelling in brown seaweed.

For other radionuclides analyzed here, Mn54, Co60, Zn65 and Ru106, the calculation of seawater activity concentration by the hydrodynamic model was potentially overestimating. This was particularly salient for Co60 and an empirical exponential decrease relationship fitted the observation data and was implemented up to 50 Km from the RP. The chemical form of Co60 is potentially specific of the reprocessing by the RP of ORANO La Hague as the source of input. The validity of this empirical relationship should be limited to 50 Km from the RP and should not be assumed for a different nuclear facility which may discharge Co radioisotopes in other chemical forms. For Mn54, Zn65 and Ru106 there was no particular correction of the calculated seawater data because there was no obvious decline of the CF values derived from the observation data in biota with distance from the RP. This did not mean that this bias was not interfering, it only indicated that it was not depending too much on distance. Furthermore the lower values of the derived CF compared to those from the literature argue that seawater activity concentrations may have been overestimated in our procedure. However, we would like to emphasize that if we underestimated the CF values (because we overestimated seawater levels), this only resulted in a vertical shift of the signal in biota (along Y-axis) but it did not alter the kinetics. In this case, the derived values for $tb_{1/2}$ should not have been affected. Again, the operational biological half-life values were the main focus of our study.

### 4.7 Perspectives

There is certainly a potential for improvements of the hydrodynamics modelling. A lower resolution, in 3D with a more accurate implementation of forcing parameters (mainly wind and bottom friction)

would be likely to change the calculated concentrations. However, we are not sure whether the residual between the observed and modelled values resulted from erroneous values calculated in seawater. Except for tritium as body water (HTO), radionuclide biological half-lives generally ranged in weeks or months. This meant a very strong smoothing of concentrations changes in biota compared to those in seawater. The two compartments transfer model was obviously a simplification and many other processes may explain the discrepancy between the observed and the calculated values. This included compartmentalization of radionuclide in biota, age/size, seasonal cycles, and so on. Another example was the case of I-129 discharges by the RP which clearly demonstrated a knowledge gap regarding its chemical speciation which largely overwhelmed the uncertainties on the hydrodynamics. Nevertheless, except for iodine-129, the actual modelling performances obtained in the present study was a starting point and it was satisfactory at least for soluble radionuclides.

The model imperfection was obvious for non-soluble radionuclides as illustrated by Co-60. Modelling the transport of radionuclides associated with particulate material is a next challenge. The realistic estimation of non-soluble radionuclides concentrations in seawater and in the sediment is a prerequisite prior to estimating their transfer to biota. Non-soluble radionuclides are candidates as potential tracers of processes (Rivier *et al.*, 2017) underlying the behavior of non-soluble pollutants in the marine environment (metals, organic compounds,…). A representation of the observed (ref ?) seasonal variation of FC between seawater and biota could also be implemented. It is also possible to build detailed radioecological hydrosedimentary dispersion model accounting for all process involved in seawater, sediment and biota. This represent a significant scientific and computation investment but represent a guideline for future studies.

Acknowledgments

The authors are deeply indebted to the numerous colleagues from IRSN, ORANO and the French Navy who were involved over decades in sampling, processing, radioactivity measurements and finally made the results of their tedious and consistent work available for this '*in silico*' study. The authors also wish to thank Dr Richard DUPONT (Naval Group, Cherbourg, France) for his contribution. This work was co-funded by the AMORAD project (French state financial support was managed by the National Agency for Research, allocated under the “Investments for the Future” framework program with reference ANR-11-RSNR-0002).

## 5 References

Bailly du Bois P, Salomon J-C, Gandon R, Guéguéniat P (1995) A quantitative estimate of English Channel water fluxes into the North Sea from 1987 to 1992 based on radiotracer distribution. Journal of Marine Systems 6: 457-481

Bailly du Bois P, Guéguéniat P (1999) Quantitative assessment of dissolved radiotracers in the English Channel : sources, average impact of la Hague reprocessing plant and conservative behaviour (1983, 1986, 1988 and 1994). Continental Shelf Research 19: 1977-2002

Bailly du Bois P, Germain P, Rozet M, Solier L (2002) Water masses circulation and residence time in the Celtic Sea and English Channel approaches, characterisation based on radionuclides labelling from industrial releases. In International Conference on Radioactivity in Environment, pp 395 – 399. Monaco

Bailly du Bois P, Dumas F (2005) Fast hydrodynamic model for medium- and long-term dispersion in seawater in the English Channel and southern North Sea, qualitative and quantitative validation by radionuclide tracers. *Ocean Modelling* **9:** 169-210

Bailly du Bois P, Dumas F, Solier L, Voiseux C (2012) In-situ database toolbox for short-term dispersion model validation in macro-tidal seas, application for 2D-model. *Continental Shelf Research* **36:** 63-82

Bailly du Bois P, Dumas F, Morillon M, Furgerot L, Voiseux C, Poizot E, Méar Y, Bennis AC (2020) The Alderney Race: general hydrodynamic and particular features. *Philosophical transactions Series A, Mathematical, physical, and engineering sciences* **378:** 20190492

Belharet M, Estournel C, Charmasson S (2016) Ecosystem model-based approach for modeling the dynamics of 137Cs transfer to marine plankton populations: application to the western North Pacific Ocean after the Fukushima nuclear power plant accident. Biogeosciences 13: 499-516

Beresford NA, Beaugelin-Seiller K, Burgos J, Cujic M, Fesenko S, Kryshev A, Pachal N, Real A, Su BS, Tagami K, Vives i Batlle J, Vives-Lynch S, Wells C, Wood MD (2015) Radionuclide biological half-life values for terrestrial and aquatic wildlife. Journal of Environmental Radioactivity 150: 270-276

Buesseler KO (2012) Fishing for answers off Fukushima. Science 338: 480-482

Carpenter LJ, MacDonald SM, Shaw MD, Kumar R, Saunders RW, Parthipan R, Wilson J, Plane JMC (2013) Atmospheric iodine levels influenced by sea surface emissions of inorganic iodine. Nature Geoscience 6: 108-111

Carvalho FP (2018) Radionuclide concentration processes in marine organisms: A comprehensive review. Journal of Environmental Radioactivity 186: 124-130

Castrillejo M, Casacuberta N, Breier CF, Pike SM, Masqué P, Buesseler KO (2016) Reassessment of 90Sr, 137Cs, and 134Cs in the Coast off Japan Derived from the Fukushima Dai-ichi Nuclear Accident. Environmental Science and Technology 50: 173-180

Colin C, Leblanc C, Michel G, Wagner E, Leize-Wagner E, Van Dorsselaer A, Potin P (2005) Vanadium-dependent iodoperoxidases in *Laminaria digitata*, a novel biochemical function diverging from brown algal bromoperoxidases. Journal of Biological Inorganic Chemistry 10: 156-166

Colpas GJ, Hamstra BJ, Kampf JW, Pecoraro VL (1996) Functional Models for Vanadium Haloperoxidase: Reactivity and Mechanism of Halide Oxidation. Journal of the American Chemical Society 118: 3469-3478

Duffa C, Bailly du Bois P, Caillaud M, Charmasson S, Couvez C, Didier D, Dumas F, Fievet B, Morillon M, Renaud P, Thébault H (2016) Development of emergency response tools for accidental radiological contamination of French coastal areas. *Journal of Environmental Radioactivity* **151:** 487-494

Douville E, Fiévet B, Germain P, Fournier M (2004) Radiocarbon behaviour in seawater and the brown algae Fucus serratus in the vicinity of the COGEMA La Hague spent fuel reprocessing plant (Goury) - France. Journal of Environmental Radioactivity 77

EDF, (2019) in French. Nuclear Power Plant Flamanville: https://www.edf.fr/centrale-nucleaire-flamanville/surete-et-environnement; NPP Paluel: https://www.edf.fr/centrale-nucleaire-paluel/surete-et-environnement; NPP Penly: https://www.edf.fr/centrale-nucleaire-penly/surete-et-environnement; NPP Gravelines: https://www.edf.fr/centrale-nucleaire-gravelines/surete-et-environnement; NPP Nogent-sur-seine: https://www.edf.fr/centrale-nucleaire-nogent-sur-seine/surete-et-environnement.

The ERA-Interim reanalysis: configuration and performance of the data assimilation system. D. P. Dee S. M. Uppala A. J. Simmons P. Berrisford P. Poli S. Kobayashi U. Andrae M. A. Balmaseda G. Balsamo P. Bauer P. Bechtold A. C. M. Beljaars L. van de Berg J. Bidlot N. Bormann C. Delsol R. Dragani M. Fuentes A. J. Geer L. Haimberger S. B. Healy H. Hersbach E. V. Hólm L. Isaksen P. Kållberg M. Kóhler M. Matricardi A. P. McNally B. M. Monge-Sanz J.-J. Morcrette B.-K. Park C. Peubey P. de Rosnay C. Tavolato J.-N. Thépault F. Vitard. First published: 28 April 2011 http://doi.org/10.1002/qj.828

Fiévet B, Plet D (2003) Estimating biological half-lives of radionuclides in marine compartments from environmental time-series measurements. *Journal of Environmental Radioactivity* **65:** 91-107.

Fiévet B, Voiseux C, Rozet M, Masson M, Bailly du Bois P (2006) Transfer of radiocarbon liquid releases from the AREVA La Hague spent fuel reprocessing plant in the English Channel. *Journal of Environmental Radioactivity* **90:** 173-196.

Fiévet B, Pommier J, Voiseux C, Bailly du Bois P, Laguionie P, Cossonnet C, Solier L (2013) Transfer of Tritium Released into the Marine Environment by French Nuclear Facilities Bordering the English Channel. *Environmental Science & Technology* **47:** 6696-6703.

Fiévet B, Bailly du Bois P, Laguionie P, Morillon M, Arnaud M, Cunin P (2017) A Dual Pathways Transfer Model to account for changes in the radioactive Caesium level in demersal and pelagic fish after the Fukushima Daï-ichi Nuclear Power Plant accident. PLoS ONE 12: e0172442

Fiévet B, Bailly du Bois P, Voiseux C, Godinot C, Cazimajou O, Solier L, De Vismes Ott A, Cossonnet C, Habibi A, Fleury S (2020) A comprehensive assessment of two-decade radioactivity monitoring around the Channel Islands. Journal of Environmental Radioactivity 223-224: 106381.

Gaudaire J-M (1999) Etude de la spéciation du 60Co dans les effluents de l'usine de retraitement de combustibles irradiés de La Hague; devenir après rejet dans les eaux de la Manche. Paris XI Orsay,

Gohin, F., 2010. Atlas de la Température, de la concentration en Chlorophylle et de la Turbidité de surface du plateau continental français et de ses abords de l'Ouest européen. Ifremer (in French. https://archimer.ifremer.fr/doc/00057/16840/14306.pdf).

Gomez LS, Marietta MG, Jackson DW. (1991) Compilation of selected marine radioecological data for the formerly utilized sites remedial action program: Summaries of available radioecological concentration factors and biological half-lives. Sandia National Laboratories, Albuquerque.

Gómez-Guzmán JM, Holm E, Niagolova N, López-Gutiérrez JM, Pinto-Gómez AR, Abril JA, García-León M (2014) Influence of releases of 129I and 137Cs from European reprocessing facilities in *Fucus vesiculosus* and seawater from the Kattegat and Skagerrak areas. Chemosphere 108: 76-84

Hou X, Aldahan A, Nielsen SP, Possnert G, Nies H, Hedfors J (2007) Speciation of 129I and 127I in seawater and implications for sources and transport pathways in the North Sea. Environmental Science & Technology 41: 5993-5999

Hou X, Povinec PP, Zhang L, Shi K, Biddulph D, Chang CC, Fan Y, Golser R, Hou Y, Ješkovský M, Jull AJT, Liu Q, Luo M, Steier P, Zhou W (2013) Iodine-129 in seawater offshore Fukushima: Distribution, inorganic speciation, sources, and budget. Environmental Science and Technology 47: 3091-3098

IAEA. (2004) Sediment distribution coefficients and concentration factors for biota in the marine environment. Technical Reports Series No 422. International Atomic Energy Agency, Vienna, p. 103.

IAEA. (2014) Handbook of Parameter Values for the Prediction of Radionuclide Transfer to Wildlife. Technical Reports Series No 479. International Atomic Energy Agency, Vienna, p. 211.

Küpper F, Schweigert N, Ar Gall E, Legendre J, Vilter H, Kloareg B (1998) Iodine uptake in Laminariales involves extracellular haloperoxidase-mediated oxidation of iodide. Planta 207: 163-171

Lazure, P., Dumas, F., 2008. An external-internal mode coupling for a 3D hydrodynamical model for applications at regional scale (MARS). Adv. Water Resour. 31 (32), 233–250.

Lyard, F., Lefevre, F., Letellier, T., Francis, O., (2006). Modelling the global ocean tides: modern insights from FES2004. Ocean Dynam. 56, 394–415.

Maro D, Vermorel F, Rozet M, Aulagnier C, Hébert D, Le Dizès S, Voiseux C, Solier L, Cossonnet C, Godinot C, Fiévet B, Laguionie P, Connan O, Cazimajou O, Morillon M, Lamotte M (2017) The VATO project: An original methodology to study the transfer of tritium as HT and HTO in grassland ecosystem. Journal of Environmental Radioactivity 167: 235-248

Muir GKP, Tierney KM, Cook GT, MacKinnon G, Howe JA, Heymans JJ, Hughes DJ, Xu S (2017) Ecosystem uptake and transfer of Sellafield-derived radiocarbon (14C). Part 1. The Irish Sea. Marine Pollution Bulletin 114: 792-804

Oms, P.-E., 2018. Tritium in Oceans: a Compilation. PANGAEA. https://doi.pangaea.de/10.1594/PANGAEA.892125.

ORANO (2019). Rapport d'information du site de La Hague TSN Report - la Hague 2019 (french only) https://www.orano.group/en/group/reference-publications

OSPAR Commission, 2014. Sixth Implementation Report: Report in Accordance with PARCOM Recommendation 91/4 on Radioactive Discharges. France. https://www.ospar.org/documents?d=7353.

RIFE-25 (2019) Radioactivity in food and the environment 2019, 25th Ed. Centre for Environment, Fisheries and Aquaculture Science on behalf of the Environment Agency, Food Standards Agency, Food Standards Scotland, Natural Resources Wales, Northern Ireland Environment Agency and the Scottish Environment Protection Agency https://www.gov.uk/government/publications/radioactivity-in-food-and-the-environment-rife-reports

Rivier, A., 2013. Dynamique des matières en suspension minérales des eaux de surface de la Manche observée par satellite et modélisée numériquement. Docteur de l'université Thesis. IFREMER DYNECO/PELAGOS et CETMEF LGCE Université de Bretagne Occidentale, Brest. (in French. https://archimer.ifremer.fr/doc/00157/26783/24884.pdf).

Rivier A, Le Hir P, Bailly Du Bois P, Laguionie P, Morillon M (2017). Numerical modelling of heterogeneous sediment transport: New insights for particulate radionuclide transport and deposition. P*aper No. 161; Coastal Dynamics Conference*; Helsingør, Denmark.

Tateda Y, Tsumune D, Tsubono T (2013) Simulation of radioactive cesium transfer in the southern Fukushima coastal biota using a dynamic food chain transfer model. J Environ Radioactivity 124: 1-12

Vives i Batlle J (2016) Dynamic modelling of radionuclide uptake by marine biota: application to the Fukushima nuclear power plant accident. Journal of Environmental Radioactivity 151, Part 2: 502-511

Vives i Batlle J, Aoyama M, Bradshaw C, Brown J, Buesseler KO, Casacuberta N, Christl M, Duffa C, Impens NREN, Iosjpe M, Masqué P, Nishikawa J (2018) Marine radioecology after the Fukushima Dai-ichi nuclear accident: Are we better positioned to understand the impact of radionuclides in marine ecosystems? *Science of The Total Environment* **618:** 80-92.

Wong G (1991) The marine geochemistry of iodine. Reviews in Aquatic Sciences 4: 45-73

Zhang LY, Hou XL (2013) Speciation analysis of 129I and its applications in environmental research. Radiochimica Acta 101: 525-540

## 6 Supplementary material

Datasets_Inventory.xlsx (Microsoft Excel file) including 3 spreadsheets: The inventory of all 136 datasets description, the coordinates of sampling locations and the annual seawater background values for Cs137 activity concentration in the English Channel.